الجمهورية الجزائرية الديمقراطية الشعبية
People's Democratic Republic of Algeria
Ministry of Higher Education And Scientific Research
University Abdelhamid Ibn Badis Mostaganem
وزارة التعليم العالي و البحث العلمي
جامعة عبد الحميد بن باديس مستغانم

Faculty of Sciences and Technology
Departement of Mechanical Engineering

كليـــــة العلـــــوم والـتكنولـــوجـــــيا
قـــسـم الـهـنـدسـة الـمـيـكـانـيـكـيـة

N° d'ordre : M……/GM/2024

Specialization: Energy

Topic

Numerical study of natural convection in a C-shaped enclosure

A dissertation submitted in partial Fulfillment of the Requirement for the Degree of Master in Mechanical Engineering

Submitted by:

- **Boudinar Cherifa**
- **Ghanes Amina Zohra**

Defended on 25/ 06 / 2024 before the jury composed of :

Chairman:	Prof. RETIEL Noureddine	***University of Mostaganem UMAB***
Examiner:	Prof. HOUAT Samir	***University of Mostaganem UMAB***
Supervisor:	Dr. SAHRAOUI Nassim Mahfoud	***University of Mostaganem UMAB***

Academic Year: 2023 / 2024

Thanking

First of all, thank God for helping us accomplish this work, and we would like to thank God for giving us the health, strength, and ambition to study and research.

And this is only a favor from God and a personal effort and struggle. We want to thank ourselves for believing in us and all the hard work we have done and for not believing in quitting. We're determined to succeed, and this is only the first step for us, and we're proud of ourselves. We would like to thank our parents, who believed in us, encouraged us, and were and will remain our support for us morally and financially. We thank them very much, and we thank our family, who also supported us. We want to thank each other a special thanks and we want to thank Committee members Prof.RETIEL Noureddine ,Prof. HOUAT Samir and supervisor Dr. SAHRAOUI Nassim Mahfoud.

thank you to all our professors and everyone who taught us a letter. Know that it is in your balance of deeds.

DEDICATION

We dedicate this work to:

My dear parents

who never stopped praying for me and helping me to achieve my goals.

My brothers

for their unfailing support.

My bestie

There are no words can describe it.

My family

for their encouragement.

my prof

For teaching and guiding me.

Amina

DEDICATION

I dedicate this work to:

My dear parents

who never stopped praying for me and helping me to achieve my goals.

My brothers

for their unfailing support.

My bestie

There are no words can describe it.

My family

for their encouragement.

my prof

For teaching and guiding me.

Cherifa

Table of contents:

Abstract:

In this work, we present a numerical study of natural convection in a C shaped cavity with the finite volume method using Fluent software.

The aim of this study is to analyze the effect of different parameters such as : different heating portions, Aspect ratio and Prandtl number on the flow structures and heat transfer. The results of the CFD analysis for the studied configuration are presented in terms of streamlines, isotherms and average Nusselt number variations. The obtained results showed that heating portions, Rayleigh number and Prandtl number have a considerable impact on the flow structures.

The results revealed that when increasing the Rayleigh number, the aspect ratio and the Prandtl number leads to an increase in the average Nusselt number and heat transfer. However, an increase in heating portion leads to a decrease in heat transfer.

Keywords: C shaped cavity, natural convection, Prandlt number effect, CFD, finite volume method

Résumé:

Ce travail propose une étude de la convection naturelle dans une cavité en forme de C par la méthode des volumes finis en utilisant le code de calcul Fluent.

L'objectif de l'étude est d'analyser l'impact des différentes portions de chauffage et de Prandtl en fonction du nombre de Rayleigh sur les diverses structures de l'écoulement et sur le transfert thermique. Les résultats de l'analyse CFD pour la configuration géométrique étudiée sont présentés sous forme de lignes de courant, de contours de température et de variations nombres de Nusselt moyens. Les résultats obtenus ont révélé que la variation des portions de chauffage, du nombre de Rayleigh et du nombre de Prandtl ont une influence considérable sur les différentes structures d'écoulement. Les résultats ont révélé que l'augmentation du nombre de Rayleigh, du rapport de forme et du nombre de Prandtl entraîne une augmentation du nombre de Nusselt moyen et du transfert de chaleur. Cependant, une augmentation de la portion de chauffage entraîne une diminution du transfert de chaleur.

Mots clés : Cavité en forme de C, convection naturelle, effet du nombre de Prandtl, CFD, méthode des volumes finis.

الملخص

يقترح هذا العمل دراسة الحمل الحراري الطبيعي في تجويف على شكل حرف C بطريقة الحجم المحدود باستخدام كود حساب فلوينت.

الهدف من الدراسة هو تحليل تأثير أجزاء التسخين المختلفة وأجزاء براندتل كدالة لرقم رايلي على هياكل التدفق المختلفة وعلى انتقال الحرارة. تم عرض نتائج تحليل CFD للتكوين الهندسي المدروس في شكل انسيابي وخطوط محيطية لدرجة الحرارة ومتوسط تغيرات رقم نسلت. أظهرت النتائج التي تم الحصول عليها أن اختلاف أجزاء التسخين ورقم رايلي ورقم براندتل له تأثير كبير على هياكل الجريان المختلفة. أظهرت النتائج أن زيادة عدد رايلي ونسبة العرض إلى الارتفاع وعدد براندتل يؤدي إلى زيادة متوسط عدد نسلت وانتقال الحرارة. ومع ذلك، فإن زيادة نسبة التسخين تؤدي إلى انخفاض في نقل الحرارة.

الكلمات المفتاحية : تجويف على شكل حرف C, الحمل الحراري الطبيعي, تاثير رقم برانتدل, عقد الفروقات, طريقة الحجم المحدود

Nomenclatures

Symbol	Definition	Unit
Cp	Heat capacity at constant pressure	J $kg^{-1}K^{-1}$
k	Thermal conductivity	J $m^{-1}s^{-1}K^{-1}$
L	Width of the cavity	m
H	height of the cavity	m
P	Non-dimensionnal pressure	
p	Pressure	Pa
T	Temperature	K
Tc	Cold wall temperature	K
Th	hot wall temperature	K
t	Dimensional time	s
u v	Dimensional velocity components along horizontal and vertical directions	ms^{-1}
U V	Non-dimensional Velocity components	
x y	Dimensional Cartésien coordinats	m
X Y	Non-dimensional Cartésien coordinats	
α	Thermal diffusivity	m^2s^{-1}
β	Thermal expansion Coefficient	K^{-1}
θ	Non-dimensional temperature	
μ	Dynamic viscosity	kg $m^{-1}s^{-1}$
ρ	Fluid density	kg m^{-3}
g	gravity	m
H	Height	m
L	Length	m
AR	Aspect Ratio	

Gr	Grashof number	
Nu	Nusselt number	
Pr	Prandtl number	
Ra	Rayleigh number	

List of figures

List of Tables

General Introduction

Heat transfer is the process by which heat is moved from one region or system to another due to a temperature difference between the two. This transfer can occur in many ways, including conduction, convection or radiation. In other terms, it's the movement of thermal energy from a hot source to a colder one, until thermal balance is reached.

A number of studies have been conducted on the subject of heat transfer by natural convection in a cavity-shaped form of c under a variety of thermal conditions.

Natural convection is a mode of heat transfer where heat is moved through a fluid, such as air or water, due to density differences caused by temperature variations.

The objective of this study is to numerically simulate a physical problem involving natural convection in a C-shaped cavity. A 2D, the top, left, and bottom walls of the enclosure are maintained at a hot temperature, while a cold square of temperature Tc is located on the adiabatic right wall of the enclosure.

We will use the gambit software to construct the geometry with mesh generation and incorporation of boundary conditions. The Fluent software used is designed by a code that is based on numerical resolution by finite volumes.

The present work will be mainly devoted to the determination of temperature contours, the streamlines and the influence of variation of heating portion, Aspect ratio and Prandtl numbers on heat transfer and flow structures.

The work is presented in three chapters. In the first chapter, a literature review on natural convection in different shaped cavities is presented. The physical, geometrical, and mathematical description, along with the corresponding assumptions and boundary conditions, is also presented.

In the second chapter, the numerical solution method, in particular the finite volume method, is presented, along with the two software packages used, GAMBIT and FLUENT.

The results of the study are presented in the third chapter. The influence of the variation of heating portion, aspect ratio and Prandtl numbers on the various flow structures and heat transfer processes.

Chapter I

Literature review and Mathematical modeling

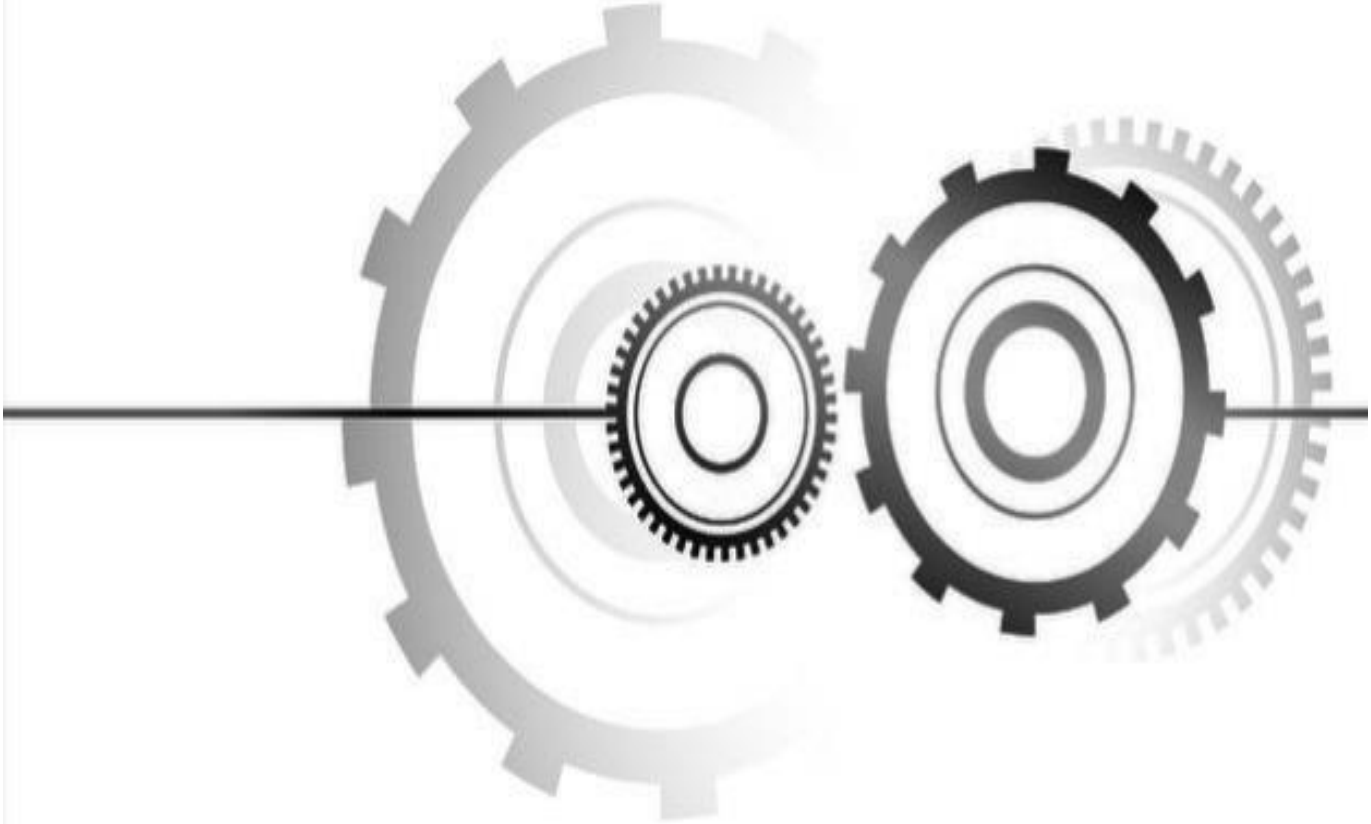

I.1 Introduction:

In this first chapter, we will present a bibliographical review of some previous studies on natural convection problems in a c-shaped enclosure, followed by the mathematical modelling of the problem to be studied.

The partial differential equations, based on the principles of conservation of mass, momentum and energy, describing the physical phenomenon with the boundary conditions taken into consideration for the studied

I.2 Bibliographical study:

In this section, a literature review on natural convection in a c is presented. The study of this problem has been carried out by numerous authors, including:

Vineet Tirth et al [1]: have studied free double-diffusive convection inside a confined C-shaped space the Boussinesq-free double-diffusive convection generated by a bulk heat source and an internal concentration in a nanofluid.The results of the study are presented in an inclined C-shaped confined space filled with nanofluid. The results can be interpreted and evaluated in terms of key variables such as Lewis number (Le = 2 to 8), Hartmann number, buoyancy ratio and Rayleigh number (Ra = 10^5 & 10^6).2023.**K Kalidasan et al [2]:** have carried out a numerical simulation of laminar natural convection of a nanofluid in an open C-shaped enclosure with an isothermal block. The variables considered are the Rayleigh number ($10^4$to 10^6) and solid hybrid particles.physics of fluid flow with a single-phase model is illustrated with streamlines, isotherms and mean Nusselt number. Heat transfer improves monotonically with increasing percentage of hybrid nanocomposites at Ra = 10^4 &10^5.2017

a study for Lattice Boltzmann Analysis of natural convection of a nanofluid in inclined C-shaped enclosures under the effect of nanoparticles Brownian motion **by Bouchmel Mliki et al [3]** The influence of pertinent parameters such as Rayleigh number, Hartmann number- The maximum value of the flux function increases with increasing Rayleigh numbers for all aspect ratios - The mean Nusselt number increases with increasing volume fraction of nanofluid , cavity, aspect ratio and cavity tilt angle.2016.

Alireza Rahimi et al [4]: presented results corresponding to the case of analyzing a C-shaped heat exchanger during natural convection are simulated using Double-MRT lattice Boltzmann method. Impacts of different effective parameters such as Rayleigh number in the range of $10^3$to 10^6, The magnitudes of the local Nusselt variation, heat transfer irreversibility and fluid friction irreversibility are dominant at the adjacent of internal active pipes and side walls. The average Nusselt number enhances as the Rayleigh number augments from $10^3$to $10^6$and the nanoparticle concentration increases from 0 to 1 vol%.

N. Makulati et al [5]: Numerical study of natural convection of nanofluid in inclined C-shaped enclosures under the effect of magnetic field the influence of pertinent parameters such as Rayleigh number ($10^3$to 10^6) and inclination angle (a) (0 to 90). The average Nusselt increased by increasing cavity aspect ratio, cavity angle and volume fraction of nanofluid. The effect of inclination angle on the heat transfer, due to the decreasing of nanofluid flow by increasing the cavity aspect ratio, decreased.2018. **M.K. Nayak et al [6]:** have carried out a simulation of natural convection with double diffusion inside a C-shaped enclosure filled with nanofluids and the efficiency of various corrugated baffle structures. The precise details of the outcomes of the present study are that streamlines intensify by 245.64%, 141.65%, 69.77%, 23.91% with rise in buoyancy ratio, Rayleigh number Ra, Lewis number and amplitude of wavy baffle respectively while that whittles down by 25.4% with rise in wave number .the heat transfer rate grows with rise in Ra. It upgrades with growing in buoyancy ratio N at high Ra while it maintains the same trend with hike in b at any Ra.2022.

lattice Boltzmann simulation of MHD natural convection of Bingham nanofluid in a C-shaped enclosure with response surface analysis was carried out by **Nur E. Jannat Asha and Md. Mamun Molla [7]** , Boundary conditions are presented in accordance with the heated, cold, and adiabatic conditions present in the cavity's various walls. Several parameters including Bingham number (Bn = 0, 0.5, 1, 1.5, 2), Rayleigh number (Ra = 10^4, 10^5, 10^6), Hartmann number and nanoparticle volume fraction. In order to gain a deeper understanding of the rate of heat transfer, it would be beneficial to consider the local Nusselt number along the three separate walls (bottom, left and top) It would appear that heat transfer decreases for the bottom wall but increases for the left and top walls when Bn, Ha It would appear that as the Ra value increases, so too does the overall decay rate. It is interesting to note that the lower wall has the lowest decay rate, while the upper wall It would appear that the upper wall has the highest rate..2023.**M.A. Mansour et al [8]**: study of mixed convection by nanofluid in a C cavity with heat and inclined magnetic field, The cavity is subjected to an inclined uniform magnetic field, and the top wall of the cavity is adiabatic and moves with a constant velocity .At L = 0.8 and 1, the increment of Ha from zero to about 40 accounts for the increase of heat transfer, and the Nusselt number reduces with the increment of Ha up to 100. For other values of L, an increment of Ha causes a decrease of the Nusselt number. **M.A.H. Mamun [9]:** The objective of this study is to investigate the effect of a magnetic field on natural convection in a C-shaped cavity filled with ferrofluid. To this end, numerical simulations have been carried out for a wide range of Rayleigh numbers (Ra =10^3, ~ 10^7) and Hartmann numbers. The results are interpreted based on streamline and isotherm patterns, as well as the average Nusselt number of the heated wall

and the average fluid temperature of the cavity.

Mostafa Mahmoodi and Hashemi, Seyed. [10]: Numerical study of the natural convection of a nanofluid in C-shaped enclosures (using the finite volume method and the SIMPLER algorithm). A parametric study was carried out and the effects of relevant parameters such as Rayleigh number ($10^5$and 10^6), aspect ratio (0.2 to 0.8) were investigated, the effect of Cu nanoparticles on heat transfer enhancement was greater for narrow enclosures than for wide enclosures**. T. Armaghani1 et al [11]:** research into MHD mixed convection flow and heat transfer in an open C-shaped enclosure using a water-copper oxide nanofluid (the governing equations were solved using the SIMPLE algorithm). The effect of several parameters such as Reynolds, Hartmann and Richardson numbers (the local Nusselt number is increased by increasing the Richardson number).The effect of a baffle on the free convection heat transfer of a water–Fe3O4 nanofluid in a C-shaped enclosure in the presence of a magnetic field is investigated numerically carried out by **Ali J. Chamkha et al [12]** , with the aid of a parametric study of the Rayleigh number, magnetic field and aspect ratio. The Nusselt number is observed to increase with an increase in the aspect ratio of the enclosure (AR, 0.1 to 0.7).

I.3 Problem description and assumptions:

I.3.1 Problem geometry:

In this section, we will study the case proposed in this topic, natural convection in a C-shaped enclosure. The top, left and bottom walls of the enclosure are maintained at a high temperature Th, and a cold square of temperature Tc is located on the adiabatic right wall of the enclosure. This forms a C-shaped enclosure. The height and width of the cavity are denoted by H. The length of the enclosure is represented by L. The aspect ratio of the enclosure is defined as follows AR = $\frac{L}{H}$.

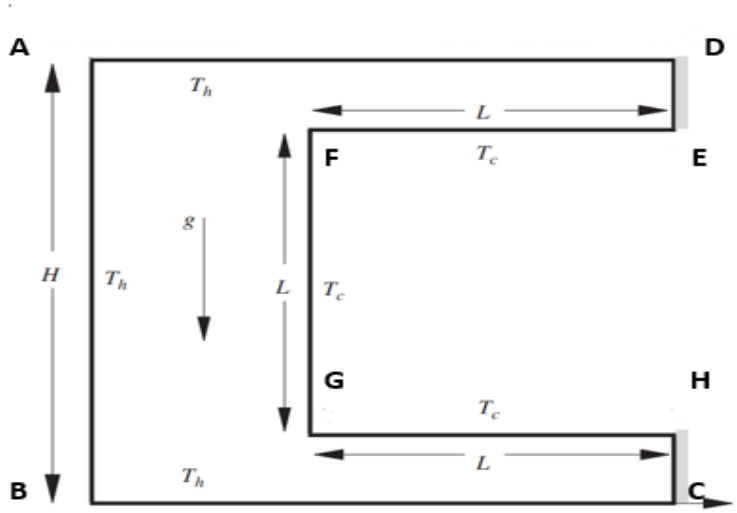

Figure. 1. A: schematic view of the C-shaped enclosure considered in the present study

I.3.2General equations:

The equations governing natural convection are:

mass balance (continuity equation), momentum balance and enthalpy (energy) balance.

a. Equation of continuity (conservation of mass):

$$\frac{\partial \rho}{\partial t} + \nabla.(\rho \vec{u}) = 0 \qquad \textbf{(1)}$$

b. Conservation equation for momentum:

$$\rho \frac{d\vec{v}}{dt} = \rho g - \nabla.p + \mu \nabla^2 \vec{v} \qquad \textbf{(2)}$$

c. Energy equation:

$$\rho Cp \frac{dT}{dt} = \nabla.\lambda \nabla T + \beta \frac{dp}{dt} + \mu \Phi \qquad \textbf{(3)}$$

I.3.3 Simplifying assumptions:

Simplifying assumptions will be useful in the mathematical modeling of our problem:

-The fluid is considered Newtonian.

- the flow is considered as steady. $\left(\frac{\partial}{\partial t} = 0\right)$

-Flow is incompressible.

- All fluid physical properties are supposed to be constant.

-Fluid flow within the cavity is laminar.

-The density variation in the fluid is approximated by the boussinesq approximation.

-Two-dimensional flow (in Cartesian coordinates x and y).

I.3.4 Mathematical formulation of the problem:

Taking simplifying assumptions into consideration, the two-dimensional equations can be written as follows:

1. ▪ Continuity equation:

$$\frac{\partial u}{\partial x} + \frac{\partial v}{\partial y} = 0 \qquad \textbf{(4)}$$

2. ▪ Equation of momentum:

Along the x-axis:

$$u\frac{\partial u}{\partial x} + v\frac{\partial u}{\partial y} = -\frac{1}{\rho}\frac{\partial p}{\partial x} + v\left[\frac{\partial^2 u}{\partial x^2} + \frac{\partial^2 u}{\partial y^2}\right] \qquad \textbf{(5)}$$

Along the y-axis:

$$u\frac{\partial v}{\partial x} + v\frac{\partial v}{\partial y} = -\frac{1}{\rho}\frac{\partial p}{\partial y} + v\left[\frac{\partial^2 v}{\partial x^2} + \frac{\partial^2 v}{\partial y^2}\right] + g\beta(T - T_0) \qquad \textbf{(6)}$$

3. ▪ Energy equation:

$$\left[u\frac{\partial T}{\partial x} + v\frac{\partial T}{\partial y}\right] = \alpha\left[\frac{\partial^2 T}{\partial x^2} + \frac{\partial^2 T}{\partial y^2}\right] \qquad \textbf{(7)}$$

I.3.5 a Dimensional formulation:

In order to reduce the above equations to a dimensionless form, it is necessary to define the following variable changes:

$$X = \frac{x}{H}\ , Y = \frac{y}{H}\ , \theta = \frac{T - T_f}{T_c - T_f}\ , U = \frac{u}{\frac{\alpha}{H}}, V = \frac{v}{\frac{\alpha}{H}}\ , P = \frac{p - P_0}{\rho\left(\frac{\alpha}{H}\right)^2} \qquad \textbf{(8)}$$

a▪ Dimensionless form of the continuity equation:

$$\frac{\partial U}{\partial X} + \frac{\partial V}{\partial Y} = 0 \qquad \textbf{(9)}$$

b. Equations of momentum:

Along the x axis:

$$U\frac{\partial U}{\partial X} + V\frac{\partial U}{\partial Y} = -\frac{\partial P}{\partial X} + Pr\left[\frac{\partial^2 U}{\partial X^2} + \frac{\partial^2 U}{\partial Y^2}\right] \qquad \textbf{(10)}$$

Along the y axis:

$$U\frac{\partial V}{\partial X} + V\frac{\partial V}{\partial Y} = -\frac{\partial P}{\partial Y} + Pr\left[\frac{\partial^2 V}{\partial X^2} + \frac{\partial^2 V}{\partial Y^2}\right] + Ra.Pr.\theta \qquad \textbf{(11)}$$

d. Energy equation:

$$U\frac{\partial \theta}{\partial X} + V\frac{\partial \theta}{\partial Y} = \left[\frac{\partial^2 \theta}{\partial X^2} + \frac{\partial^2 \theta}{\partial V^2}\right] \qquad \textbf{(12)}$$

I.3.6 Boundary conditions:

Solving the system of equations obtained above requires the incorporation of appropriate boundary conditions for the dynamic and thermal fields.

Table I.1: Boundary conditions

Walls	Geometric boundary	Dynamic conditions
AD	Y=1 0<X<1	U= 0, V=0 $\theta = \theta_h$
AB	X=0 0<Y<1	U= 0, V=0 $\theta = \theta_h$
BC	Y=0 0<X<1	U= 0, V=0 $\theta = \theta_h$
EF	Y=0.7 0.6<X<1	U= 0, V=0 $\theta = \theta_c$
FG	X=0.6 0.3<Y<0.7	U= 0, V=0 $\theta = \theta_c$
GH	Y=0.3 0.6<X<1	U= 0, V=0 $\theta = \theta_c$
DE	X=1 0.7<Y<1	U= 0, V=0 $\frac{\partial T}{\partial X}$ =0(Adiabatic)
CH	X=1 0<Y<0.3	U= 0, V=0 $\frac{\partial T}{\partial X}$ =0(Adiabatic)

I.4 Boussinesq approximation and dimensionless numbers:

I.4.1 Boussinesq approximation:

The Boussinesq approximation introduces the assumption of incompressibility for the flow and considers density variations to be negligible at the levels of all terms of the momentum equations **(ρ = ρ0)**, with the exception of the equation of transverse motion. In practice, this assumption involves simplifying the equation of fluid state by linearizing the expression of ρ as a function of temperature variation T as follows.

$$\boldsymbol{\rho = \rho_0 [1 - \beta(T - T_0)]} \text{ .....(13)}$$

Where: $\boldsymbol{\rho_0}$: density of fluid at reference temperature $\mathbf{T_0}$

$\boldsymbol{\beta}$: coefficient of expansion at constant pressure

I.4.2 Dimensionless numbers:

a. Rayleigh number:

It's a dimensionless number that also characterizes heat transfer within a fluid. Within a fluid. This number is used in fluid mechanics. Less than one value critical value of 2000, heat transfer is by conduction; above this value, free convection becomes important. It is defined as follows:

$$\mathbf{Ra = Pr \times Gr} \quad \textbf{or} \quad \mathbf{Ra = \frac{g.\beta.\Delta T.H^3}{\nu.\alpha}} \text{ .....(14)}$$

b. Grashof number

It describes the relationship between the natural convectional heat effects and the viscous effects

$$\mathbf{Gr} = \frac{\mathbf{g}.\boldsymbol{\beta}.\Delta\mathbf{T}.H^3}{\boldsymbol{\nu}^2} \quad \text{.....(15)}$$

c. Prandtl number:

This is a dimensionless number. It represents the ratio between momentum diffusivity (or kinematic viscosity) and thermal diffusivity. It is defined as follows

$$\mathbf{Pr} = \frac{\boldsymbol{\rho}.\mathbf{v}.\mathbf{Cp}}{\boldsymbol{\lambda}} = \frac{\mathbf{v}}{\boldsymbol{\alpha}} \quad \text{.....(16)}$$

The Prandtl number is a dimensionless number. It is defined as the ratio of the diffusivity of momentum in other words, the ratio of kinematic viscosity to thermal diffusivity.

d. Nusselt number:

The Nusselt number is a dimensionless number often used in heat transfer applications; it describes the heat flow between a plate and the fluid surrounding it. It shows the relationship between the actual flux that the plate transmits to the fluid and the flux that would be transmitted in a regime of pure conduction.

$\boldsymbol{\Phi convectif} = -\boldsymbol{\lambda}\frac{\partial T}{\partial X} = \boldsymbol{hc}(\boldsymbol{Tp} - \boldsymbol{T0})$;

$\boldsymbol{\Phi conductif} = \boldsymbol{\lambda}(\boldsymbol{Tp} - \boldsymbol{T0})\ \boldsymbol{\lambda} \times \boldsymbol{L}\ \boldsymbol{Nu}$

$\boldsymbol{\Phi convectif}\ \boldsymbol{\Phi conductif} = -\boldsymbol{\lambda}\frac{\partial T}{\partial X} = \boldsymbol{\lambda}(\boldsymbol{Tp} - \boldsymbol{T0})\ \boldsymbol{\lambda} \times \boldsymbol{L} = \boldsymbol{hc} \times \boldsymbol{L}$

I.5 Conclusion:

In this chapter, we presented a literature review on natural convection in different shaped enclosure. We have also presented the two-dimensional equations of natural convection that apply to our problem.

In the next chapter, we present the numerical methods for solving these equations, in particular the finite volume method and the computational tools used in this study (Gambit and Fluent).

Chapter II

Description of the Equation Solving Method and Numerical tools

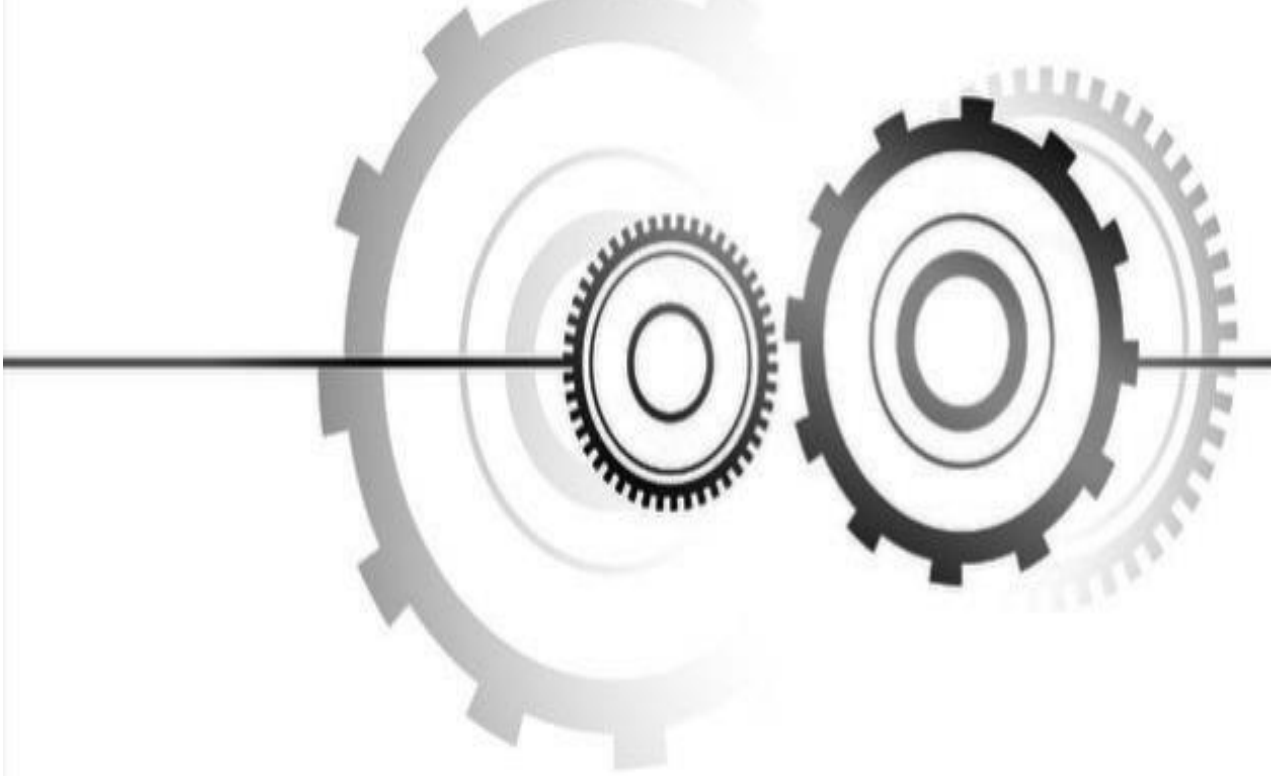

II .1 Introduction:

Simulation is defined as the use or resolution of models of a given system to study its behavior in a specific context.

It is the logical continuation of modeling, which is the first approach to simulation, which takes the form of a computer program or tool using a numerical method of method of discretizing the governing equations. This set of tools is called a simulation environment

In this work, we have opted for a numerical approach using the commercial code FLUENT, which is based on the finite volume method for discretizing the governing equations.

In this chapter, we present the method for numerically solving these equations and the tools used.

II.2 Finite volume methods (FVM):

The finite volume method is an approach used in CFD. It consists in defining a grid of points called nodes within the computational domain. Each node is surrounded by an elementary surface on which the partial differential equations will be integrated.

The finite volume method is a discretization method for conservation laws. It is based on the writing of physical balances. This method consists in discretizing the integral form of the problem to be solved on each of the cells, called control volumes. One of the main difficulties that can be encountered is the estimation of flows at the boundaries of each control volume when implementing this technique.

II.3 Description of Gambit software:

3.1 Gambit preprocessor:

The Gambit software is a preprocessor for creating or importing simple or complex geometries (surface or volume) in 2D or 3D, simple or complex.it can create Several mesh types (structured, unstructured or hybrid) in Cartesian, polar, Cartesian, polar, cylindrical or axisymmetric coordinates and specify the type of material (fluid or solid) at the user's discretion. The preprocessor also enables you to define appropriate boundary conditions at the boundaries of the calculation domain. It also features numerous extraction capabilities, enabling its meshes to be used by industrial software such as FLUENT. The Gambit combines three essential functions:

- Problem geometry definition.
- Meshing and verification.
- Definition of boundaries (boundary conditions) and definition of computational domains.

II.3.2 Gambit interface and steps:

II.3.2.1. Launching Gambit:

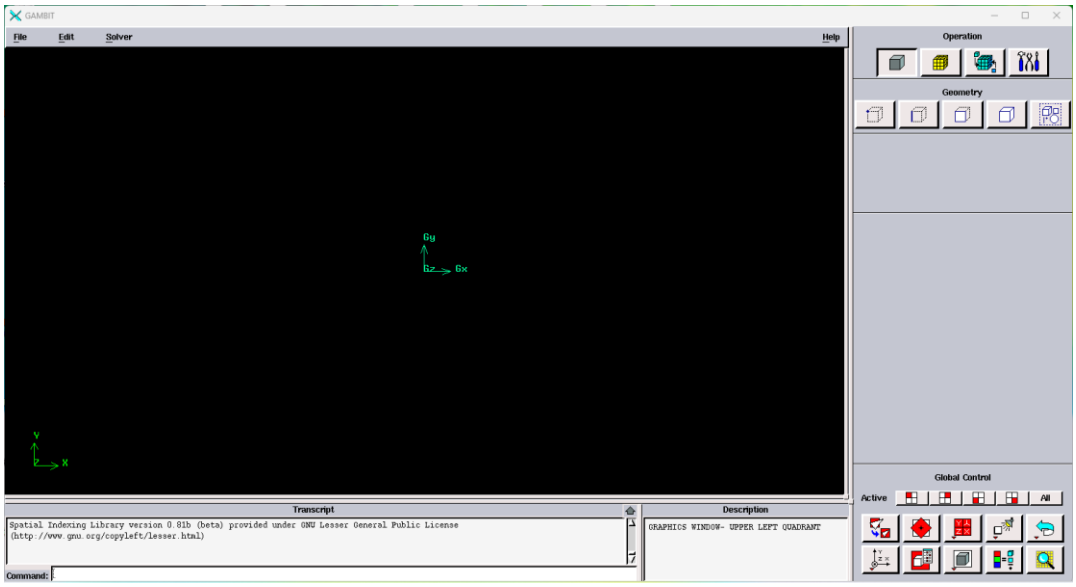

General menu

Secondary menu

Figure II.1: Gambit interface

II.3.2.2. Construction of the geometry

creating points 2D

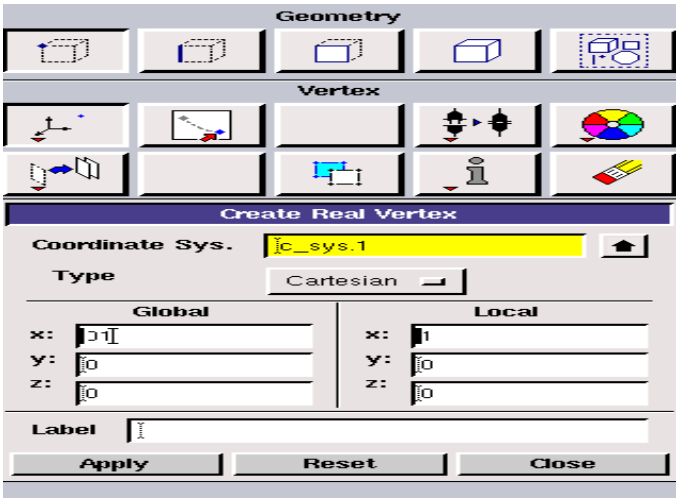

Figure II.2: Geometry construction

II.3.2.3. Mesh generation

In our case, we use a structured mesh with interval size deferent to specify the flows on the enclosure.

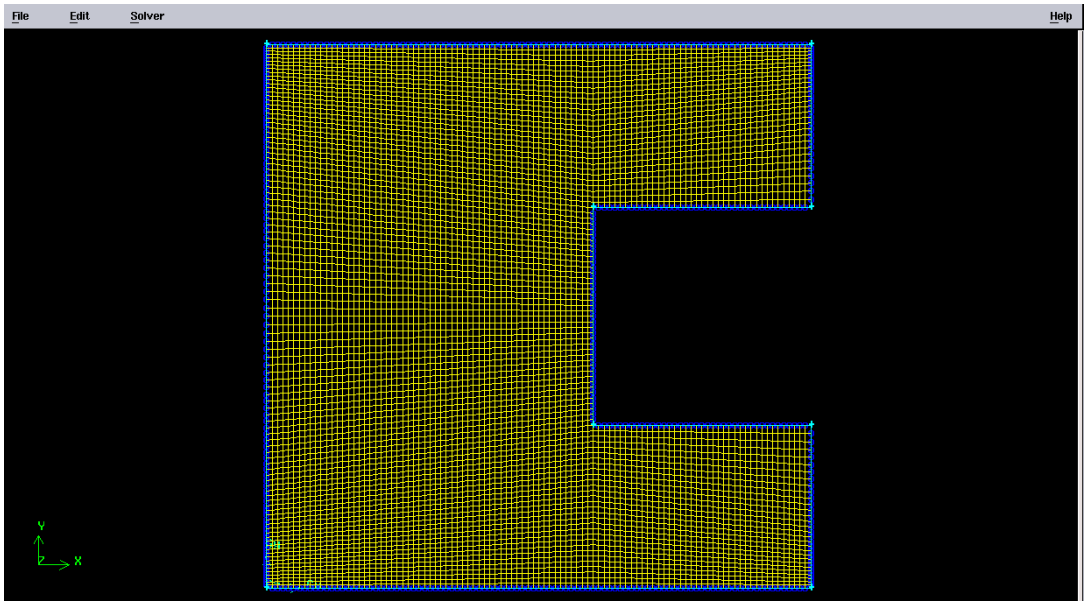

Figure II.3: Mesh generation

II.3.2.4. Boundary conditions

The following figure summarizes the various conditions that can be imposed for air flow in a air flow in an entrained square cavity.

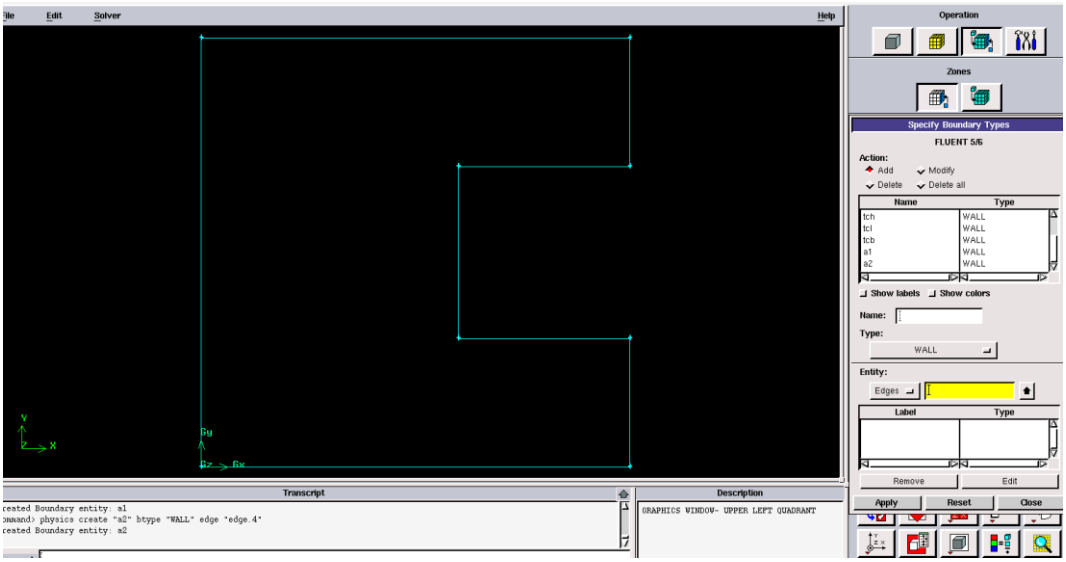

Figure II.4: Incorporation of boundary conditions

II.3.2.5. Exporting the Gambit mesh:

Once the geometry and boundary conditions have been created, the mesh is exported to the Soveur Fluent following the step: File → export → mesh

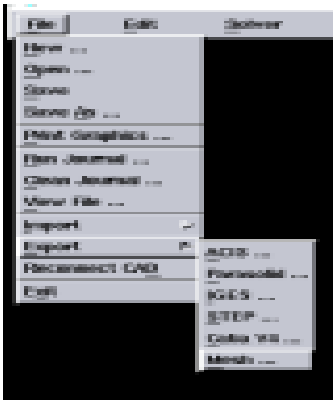

Figure II.5: Mesh export.

It requires the mesh to be exported in " Msh " format for fluent to read it and use it after saving, as follows:

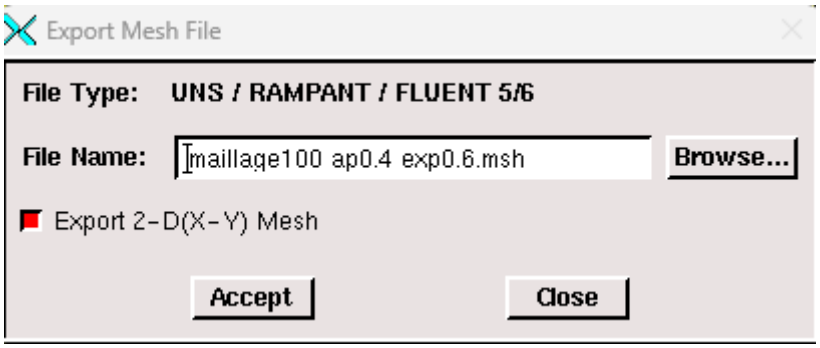

Figure II.6: Recording the mesh

II.4. FLUENT software:

II.4.1 Definition of fluent:

Fluent is a commercial CFD code widely used in industry. It can be used to solve fluid flow and heat transfer for different types of problems. For example, it can calculate the lift of an aircraft wing, the drag of a car, the cooling of electronic circuits by electronic circuits...etc.

II.4.2. Fluent solver steps:

II.4.2.1. Launch Fluent:

When starting the Fluent software, you must select the dimensions of the calculation domain

(2D or 3D), and whether the software should use single or double precision.

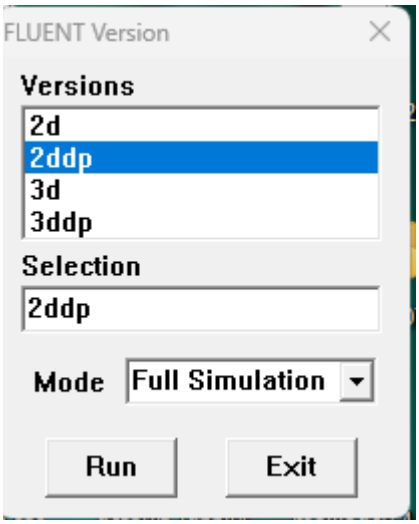

Figure II.7: distinguishing the 2ddp calculation domain

II.4.2.2 Importing the geometry:

To begin the study, we need to import the file (*.msh) generated under Gambit by the following step: File → Read → Cas

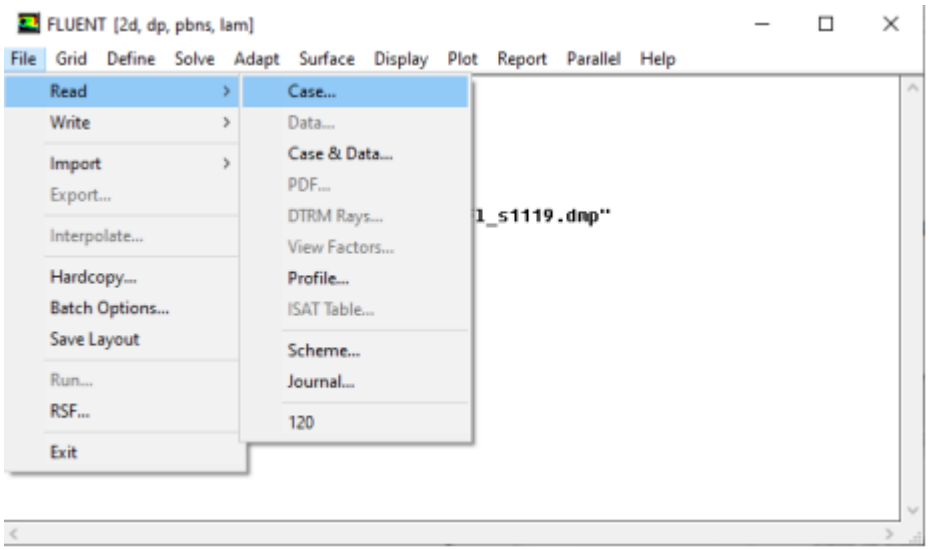

Figure II.8: Importing geometry.

The main menu we'll be using is the Grid menu.

II.4.2.3. Mesh verification:

Allows you to check the imported mesh for deformations: Grid → Check

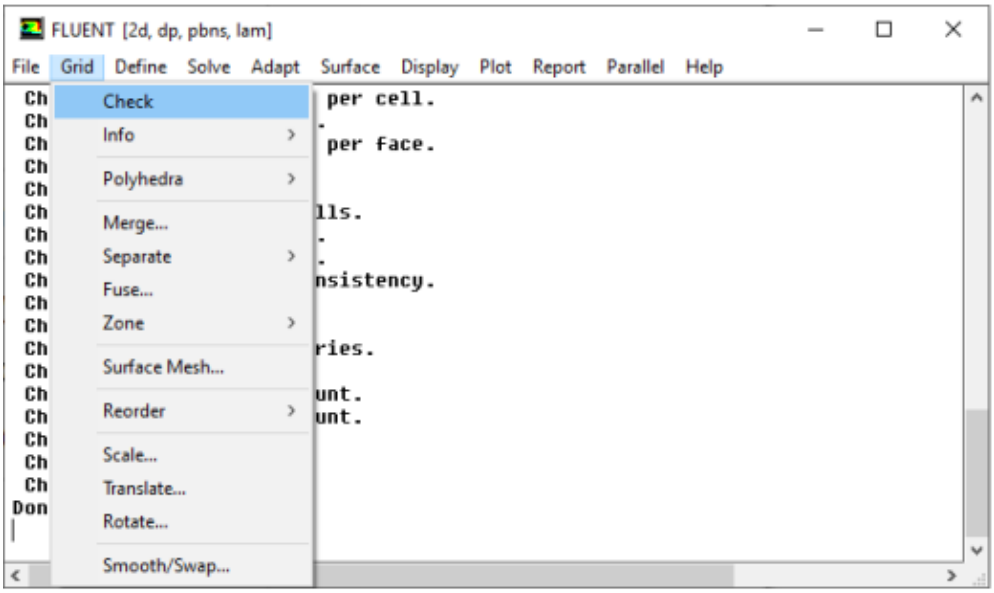

Figure II.9: Mesh verification

II.4.2.4. Checking units and dimensions:

We need to check that the dimensions and units displayed satisfy the dimensions of the physical model in our case: Grid → Scale

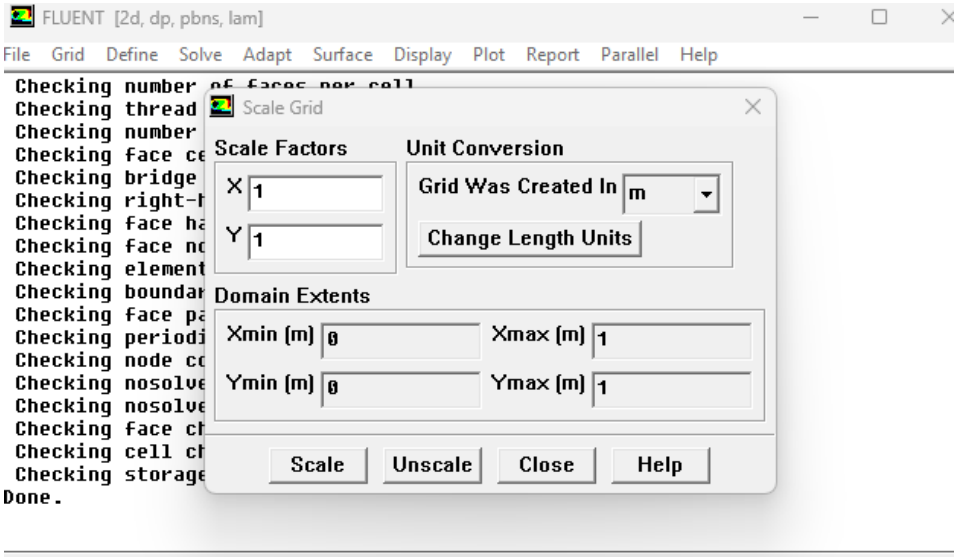

Figure II.10: Checking dimensions and units

II.4.3 Model definition

II.4.3.1. Solver selection:

This menu is used to select the type of solver you wish to use (implicit scheme, steady-state implicit scheme, steady state, 2D configuration...) defined as follows:

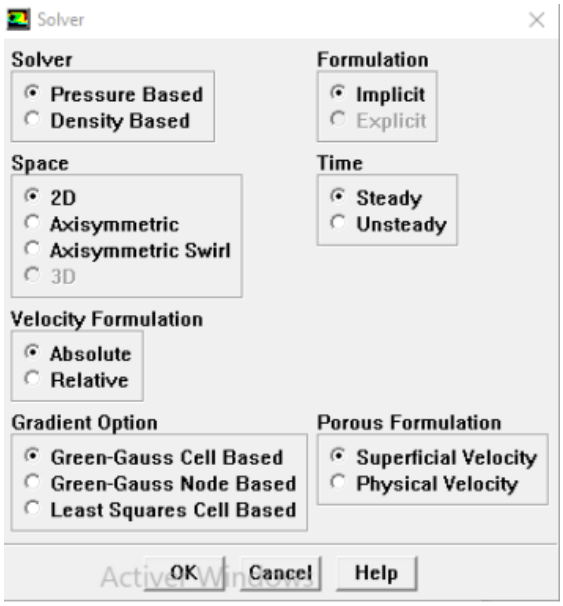

Figure II.12: Choice of solver

II.4.3.2. Choice of flow regime:

Different flow models exist. These include laminar and turbulent flows.

Define → Models → Viscous

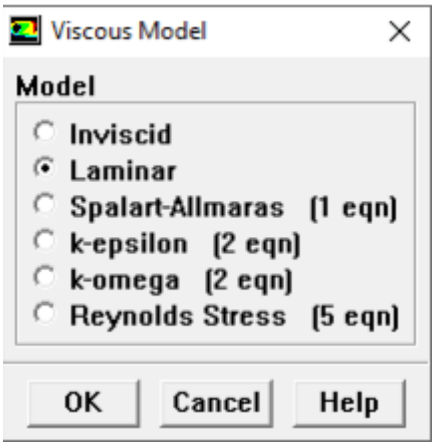

Figure II.13: Laminar model selection

In the Models menu which is to be used according to the problem statement.

II.4.3.3. checked energy:

Define → Models → energy

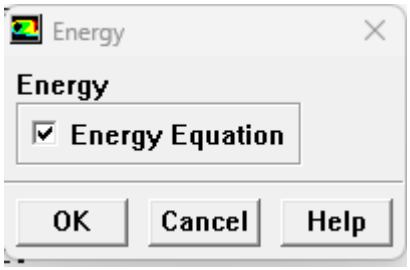

II.4.4 Equipment definition

II.4.4.1. Material characteristics:

Fluid selection is defined as follows: Define – Materials

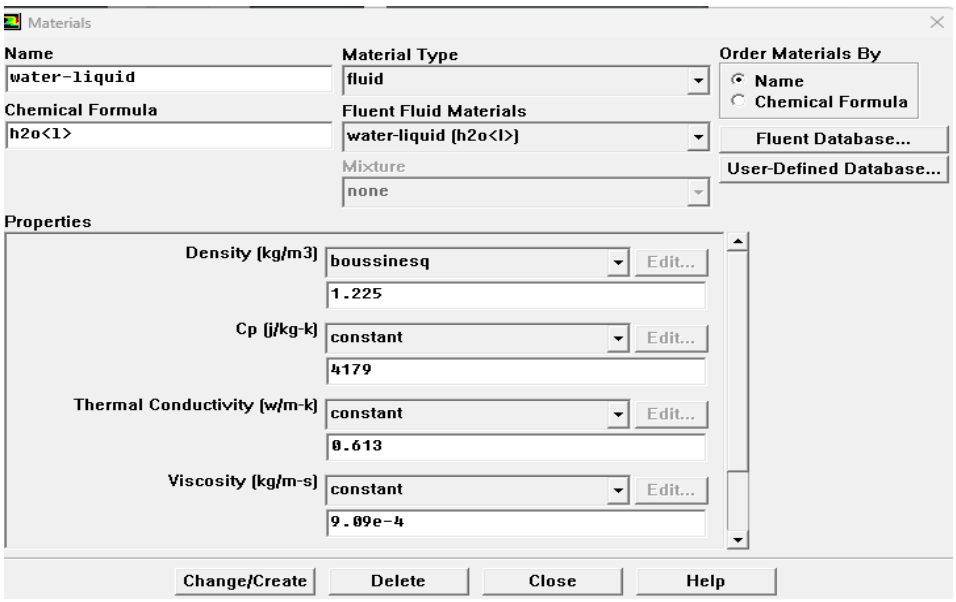

Figure II.14: Material characteristic

II.4.4.2. Operating conditions:

This activity allows you to set the operating conditions:

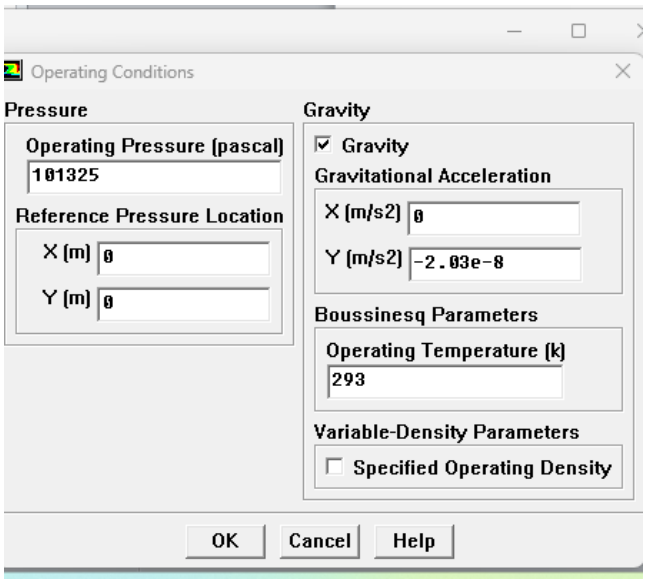

Figure II.15: choice of operating conditions

II.4.4.3. Boundary conditions:

It is necessary to set the values of the boundary conditions of the problem to be treated:

Define → Boundary conditions

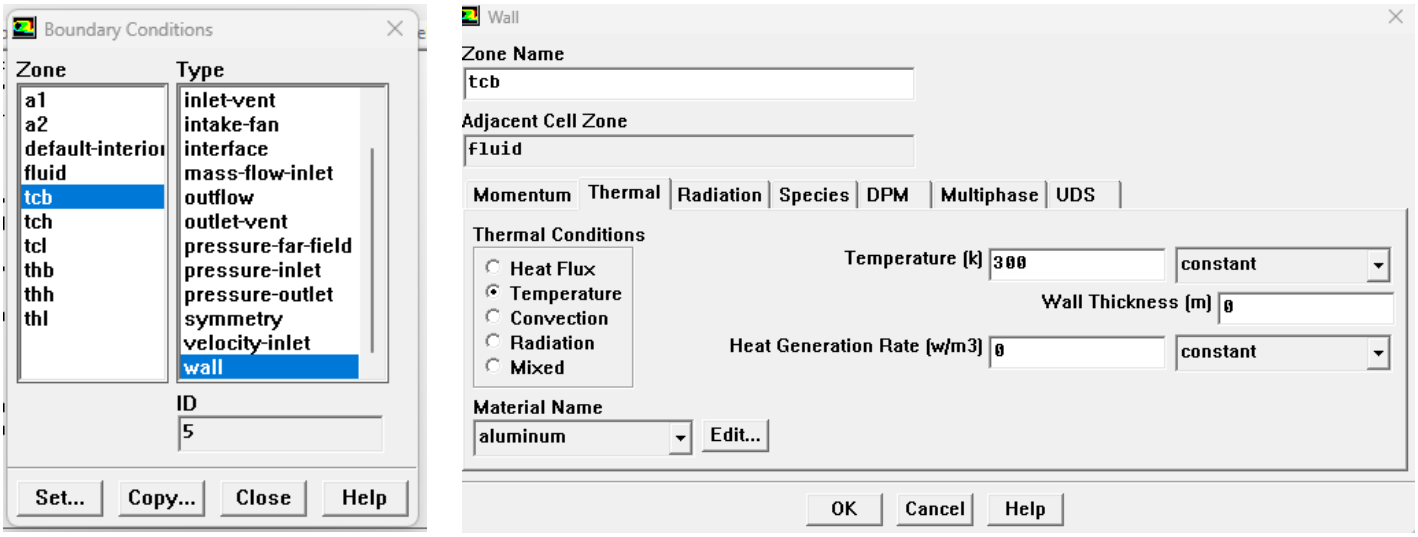

Figure II.16: Input speed (boundary conditions)

The Solve menu is used to determine the various elements required to initialize Fluent solver

II.4.5 The solver:

III.4.5.1. Checking the solution:

This step enables us to estimate the discretization schemes, as well as the choice of equation order and algorithm (or solution choice). Solve - Control –Solution

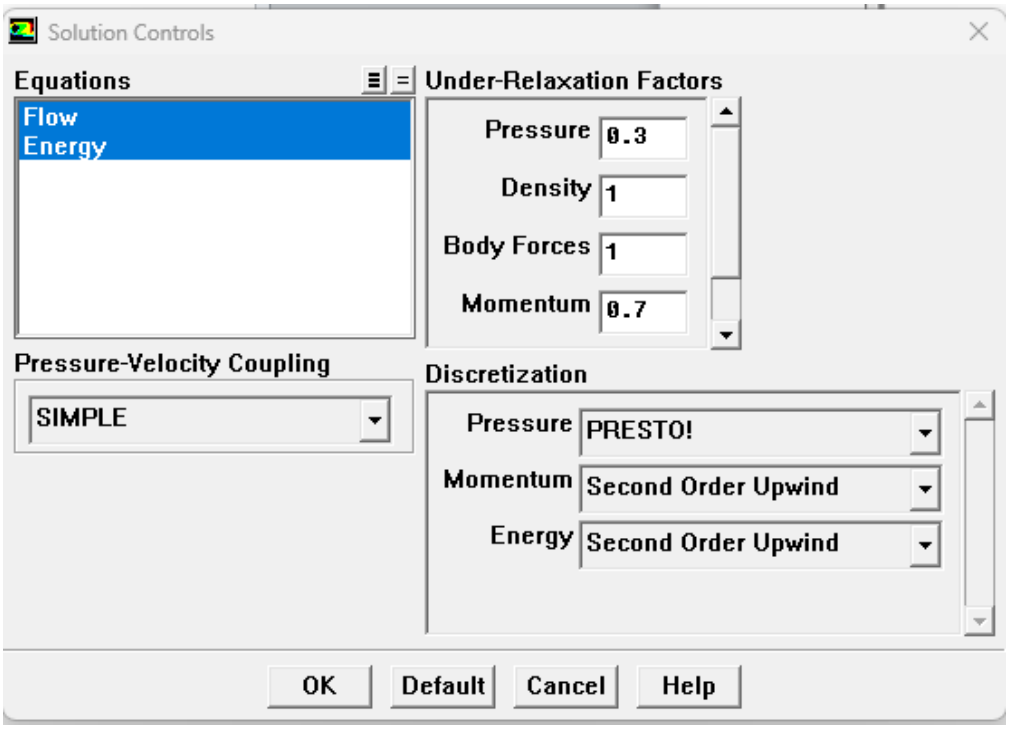

Figure II.17: Choice of equation order

II.4.5.2. Initialize:

This option is used to initialize the calculation: Solve → Initialize → Initialize

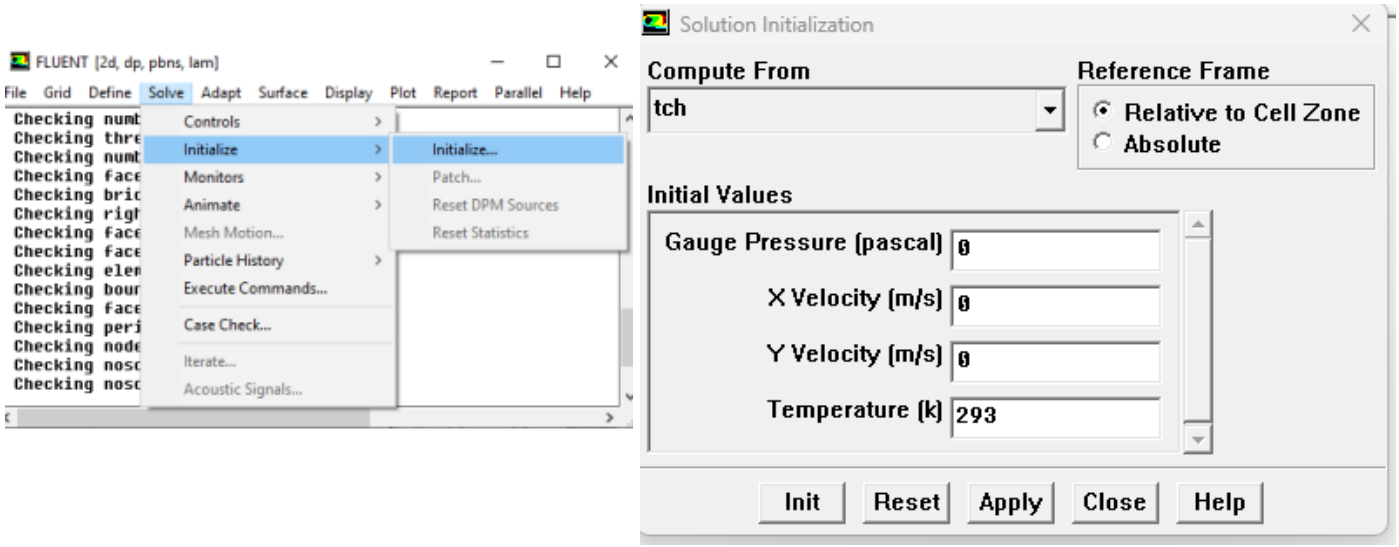

Figure II.18: Calculation initialization

II.4.5.3. Choice of convergence criteria:

The convergence criteria that must be considered in order for

Calculations are stopped: Solve → Monitors → Residual

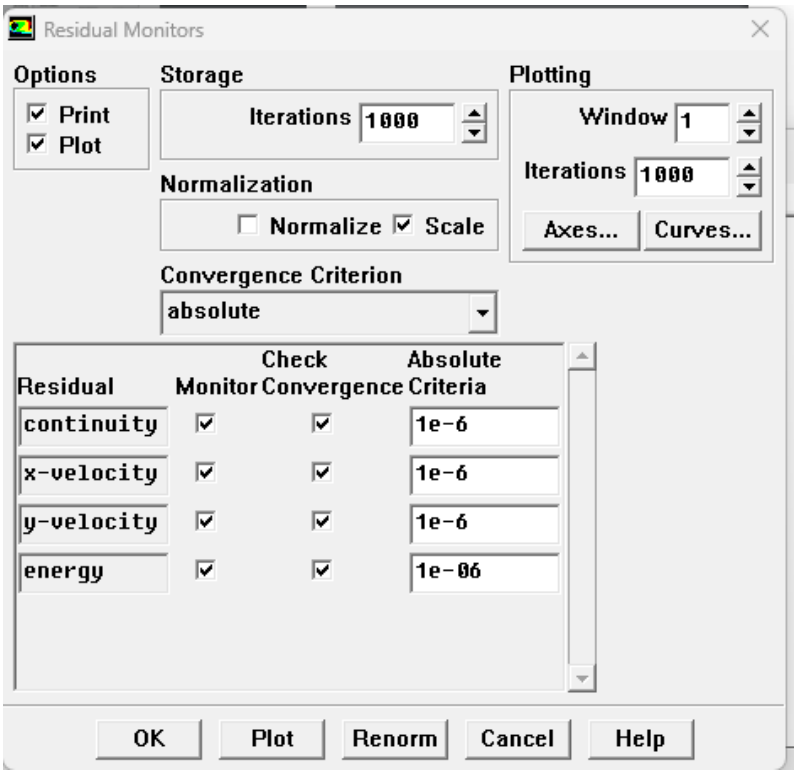

Figure II.19 : Choice of convergence criteria

Note: To display convergence on screen during calculations in the form of a graph the Plot option must be activated.

II.4.5.4. Starting convergence calculations:

Before starting calculations, you must first select the number of iterations: solve → iterate

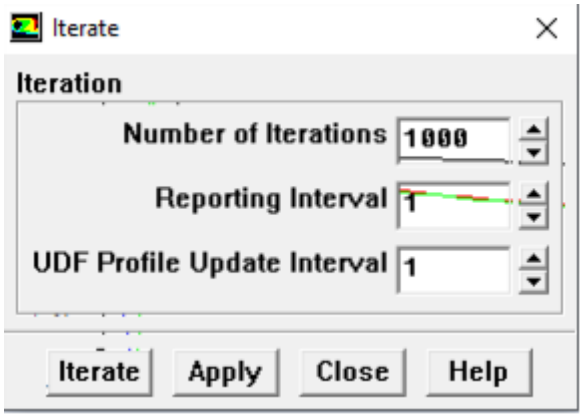

Figure II.20: Choice of number of iterations

II.4.5.5. Evolution of calculation residuals:

The calculation converges when the residual is stable,

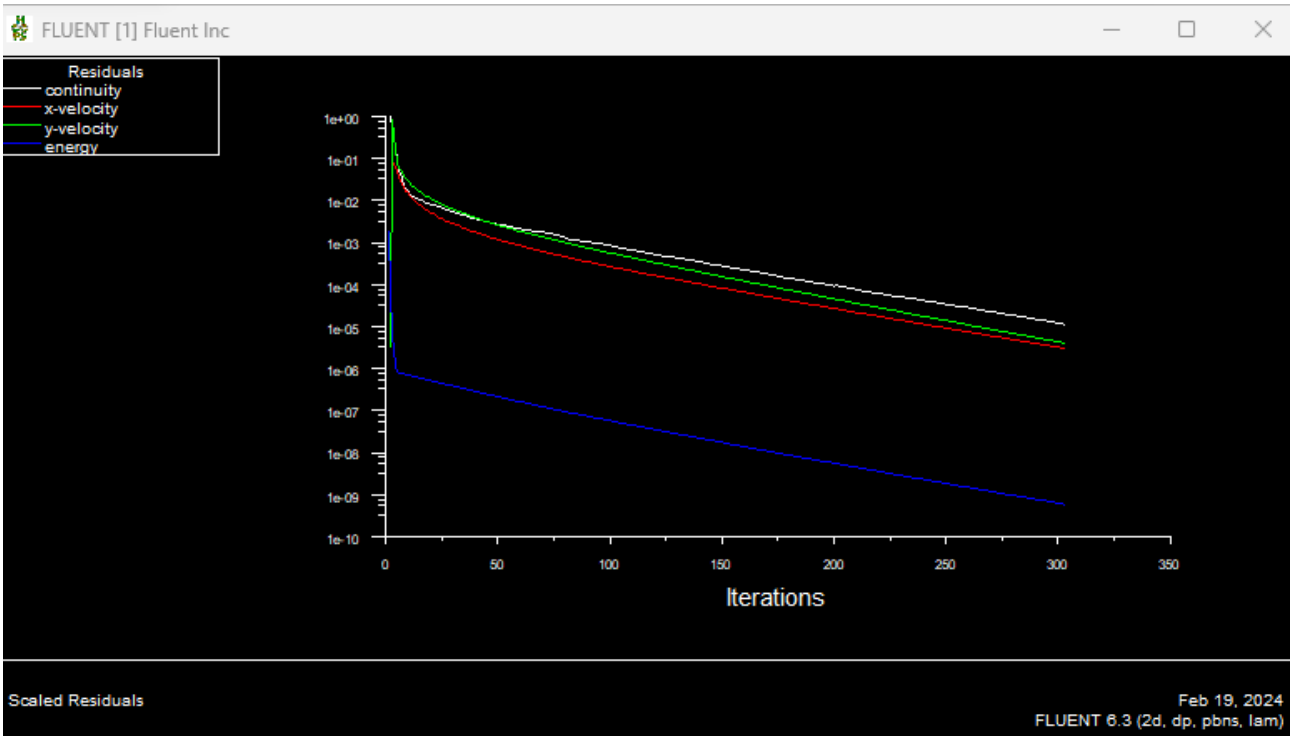

Figure II.21: Evolution of calculation residuals for 100x100 mesh

The results can be visualized and analyzed using the post-processing tool provided by Fluent. These features are mainly:

❖ Display

1. The first Contours menu, which studies variable variations in the form of streamlines velocity profile: Display → Contours...

2. The second vectors menu, where values are explained by vectors for speed vectors: Display → Vectors

❖ Surface

Surface: visualization of mesh areas (lines, planes, etc.).

Surface allows you to create lines or planes in the geometry from points.

❖ Plot

Plot offers the potential to create 2D graphs for all variables on the lines or plane.

II.5 Conclusion:

In this chapter, we have solved the procedure for a physical problem on the gambit /fluent software, from the creation of the geometry, mesh generation, file processing on gambit to the definition of solution conditions and the visualization and analysis of results in fluent.

In the next chapter results will be presented and discussed in details.

Chapter III

Results and discussions

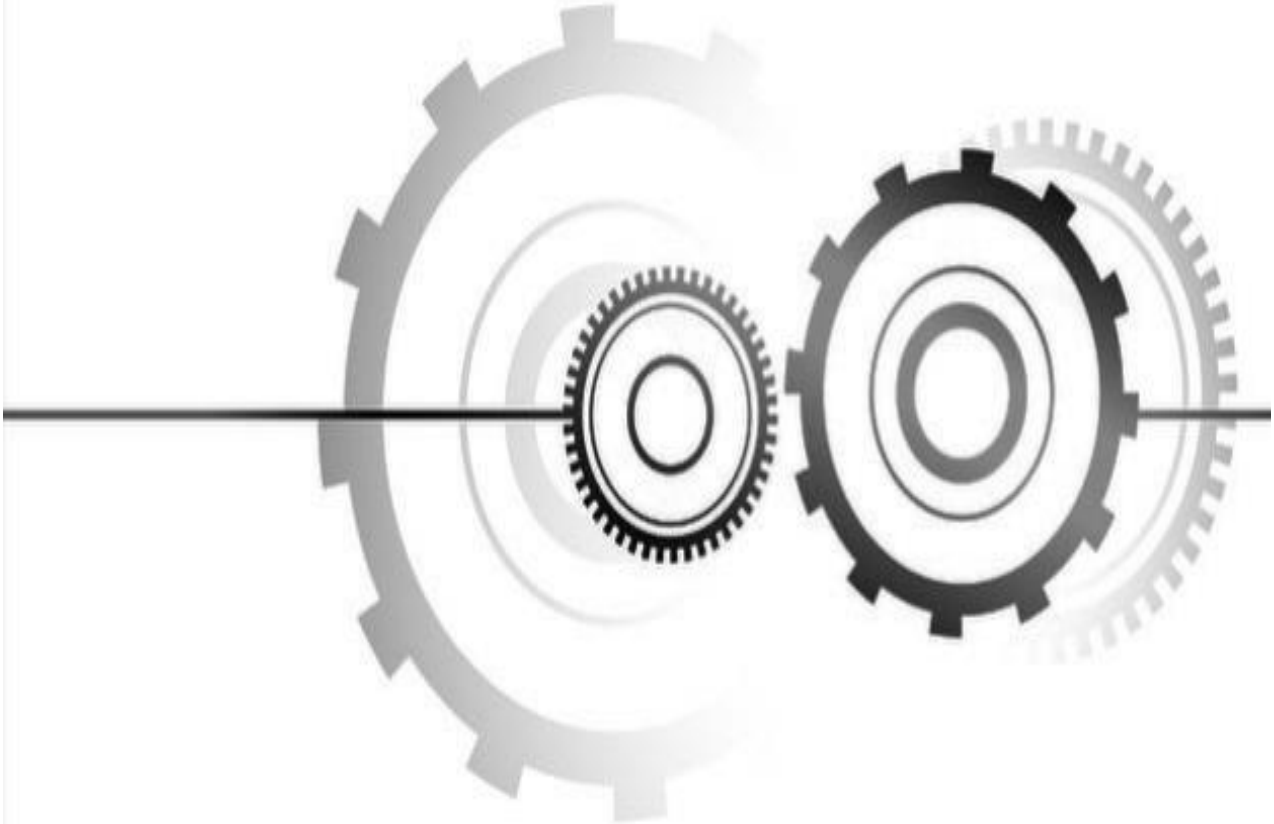

III.1. Introduction:

In this section, the study begins with a numerical validation of the studied physical problem involving natural convection in a C-shaped cavity, the top, left and bottom walls of the enclosure are maintained at a high temperature T_h, and a cold square of temperature T_c is located on the adiabatic right wall of the enclosure.

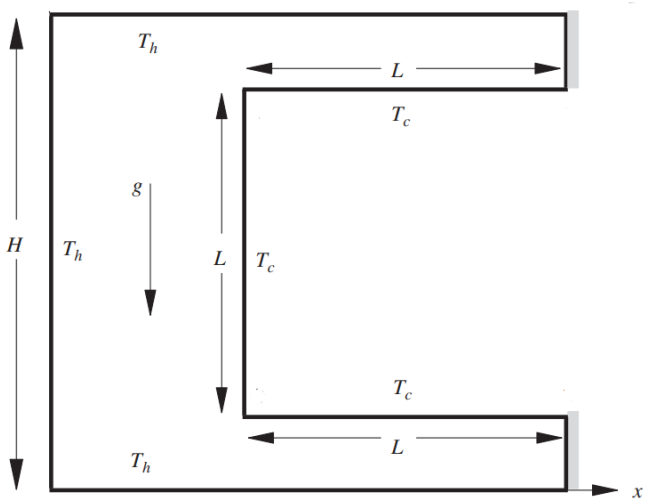

Figure III.1: shown schematically

Firstly, we will present the results of a mesh study that has been carried out for the case of natural convection in a c-shaped cavity. The results will be validated and compared with those found in the literature.

Secondly, results will be compared with the results found on the literature using the selected mesh.

Finally, the influence of heating portion, the aspect ratio and Prandtl number on the different flow structures, in terms of streamlines, isotherms, and the average Nusselt number will be presented and discussed.

The study will be carried out for numbers of Rayleigh (10^3, 10^4 , 10^5)for aspect ratios ranging from 0.2 to 0.8 and for Prandtl numbers ranging from 0.1 to 10.

III.2Numerical validation:

III.2.1 Mesh selection:

A mesh study has been carried out for a C shaped enclosure case where Rayleigh number values varying from $10^4$and 10^5, Prandtl number equal to 6.2. Simulations were carried out using several mesh sizes (40×40, 60×60, 80×80, 100×100,120×120). The choice of mesh must be justified by the convergence and precision of the Nusselt number values.

Based on the results obtained, a (100x100) mesh is adopted for the current computation.

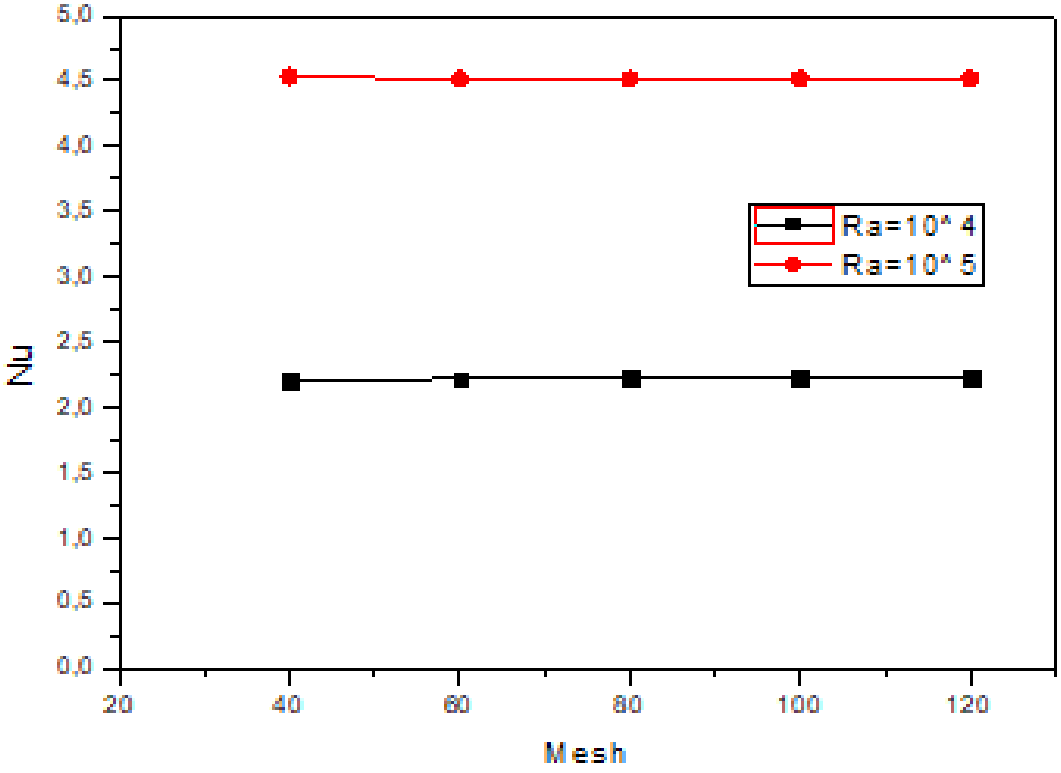

Figure III.2: Mesh study for natural convection (Ra = 10^4 and 10^5)

III.2.2 Physical validation:

We have compared the results obtained with those found in the literature

Table III.2: 1 Validation of results for the case of natural convection (Ra =10^4 and 10^5) and Pr = 6.2

Ra	Present work	M. Mahmoodi et al [10]
Nu (Ra=10^4)	1.3238	1.37
Nu (Ra=10^5)	2.4736	2.44

- For Ra=10^4 the error is 3.3%.
- For Ra =$10^5$the error is 1.3%.
- For Rayleigh numbers of 10^4 and 10^5, the maximum error does not exceed 4%, which means that our results are in good agreement with the literature.

III.3Results and discussions:

In this section, we will study the case proposed in this topic, natural convection in a C-shaped enclosure. The top, left, and bottom walls of the enclosure are maintained at a hot temperature Th, and a cold box with temperature Tc is imposed on the fixed right walls of the enclosure, the rest of the walls are adiabatic. (Figure III.3).

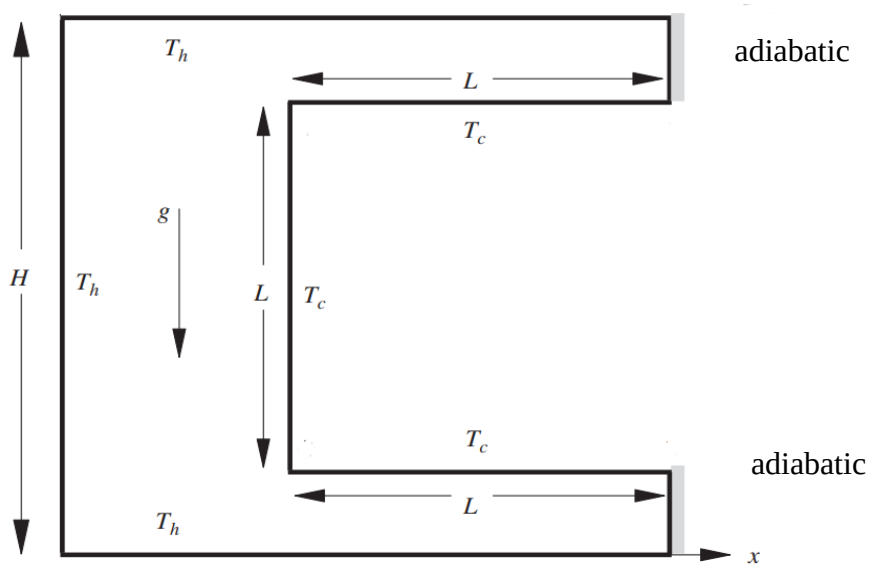

Figure III.3. Physical configuration of the studied phenomenon

III.3.1 Study of the influence of the Heating portion:

In this section, the influence of the heating portion will be examined, the aspect ratio being fixed in 0.4 while varying the Rayleigh number by Ra = (10^3, 10^4,10^5) and varying the heating portion by Ɛ= (0.2, 0.6, 0.8) with a Prandtl number equal to 6.2.

Figures III.4: shows the isotherms as a function of Rayleigh number for heating portions from Ɛ = 0.2 to 1, for an aspect ratio of AR=0.4.

It seems that an increase in the Rayleigh number may result in an increase in the flow motion, buoyancy force, and temperature gradient.

From the isotherms in the figures, it appears that for Ra=10^3, for all heating portions, the isotherms are almost parallel, this suggests that conduction is the dominant heat transfer mode inside the enclosure. Conversely, as the Rayleigh number increases, a deformation of the isotherms is observed. The fluid in contact with the cold wall flows downwards because its density is higher at low temperatures. On the other hand, the fluid in contact with the hot wall flows upwards because it is very light, and this is because its density is lower at higher

temperatures. This is due to an increase in the buoyancy forces and temperature gradient, so convective heat transfer is particularly important for higher Ra numbers.

It is also observed in the heating portion that the different way heat is distributed in the emission affects the deformation motion, as shown at Ɛ =0.2.

It is interesting to note that a thermal plume is formed between the cold and the hot walls located in the lower right part of the cavity as a function of the increasing Rayleigh number.

Figure III.5: shows the streamlines as a function of Rayleigh number for heating portions from Ɛ = 0.2 and 1 to AR=0.4 respectively

It can be observed that an increase in the Rayleigh number results in alterations of the streamlines form, giving rise to the formation of vortices rotating in a clockwise direction, as observed in all cases of heating. The vortex exhibits uniform rotation when the Rayleigh number is low, but as it increases, we notice the formation of two counter-rotating vortices. For Ra = 10^4, the flow pattern is symmetrical. For the case Ra = 10^5, the vortex splits into two counter-rotating vortices. The larger vortex rotates clockwise and is located on the left side of the enclosure, while the smaller counter-clockwise rotating vortex is located under the cold wall.

Thus, as the Rayleigh number increases, the dominance of natural convection increases and, at the same time, the flow structure changes.

In **Figure III.6**: Variation of average Nusselt number with the Rayleigh number for different heating portions Ɛ =0.2, Ɛ =0.6, Ɛ =1. We observe that the average Nusselt number decreases as the number of heating portions increases, and that the variation in the Nusselt number increases as the Rayleigh number increases.

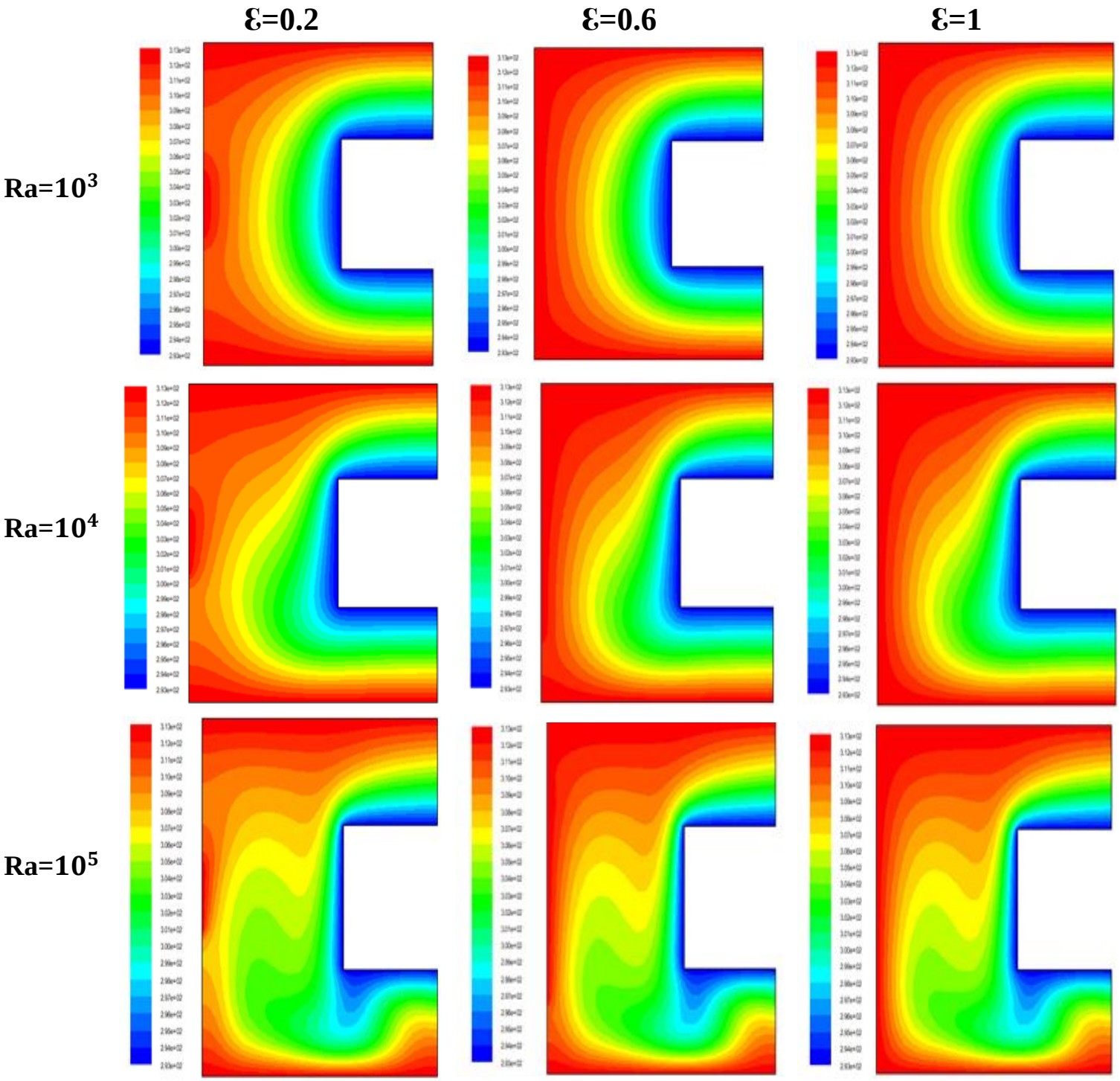

Figure III.4: isotherms for (Ɛ =0.2,0.6,1 to Ra=10^3 at 10^5) and AR=0.4

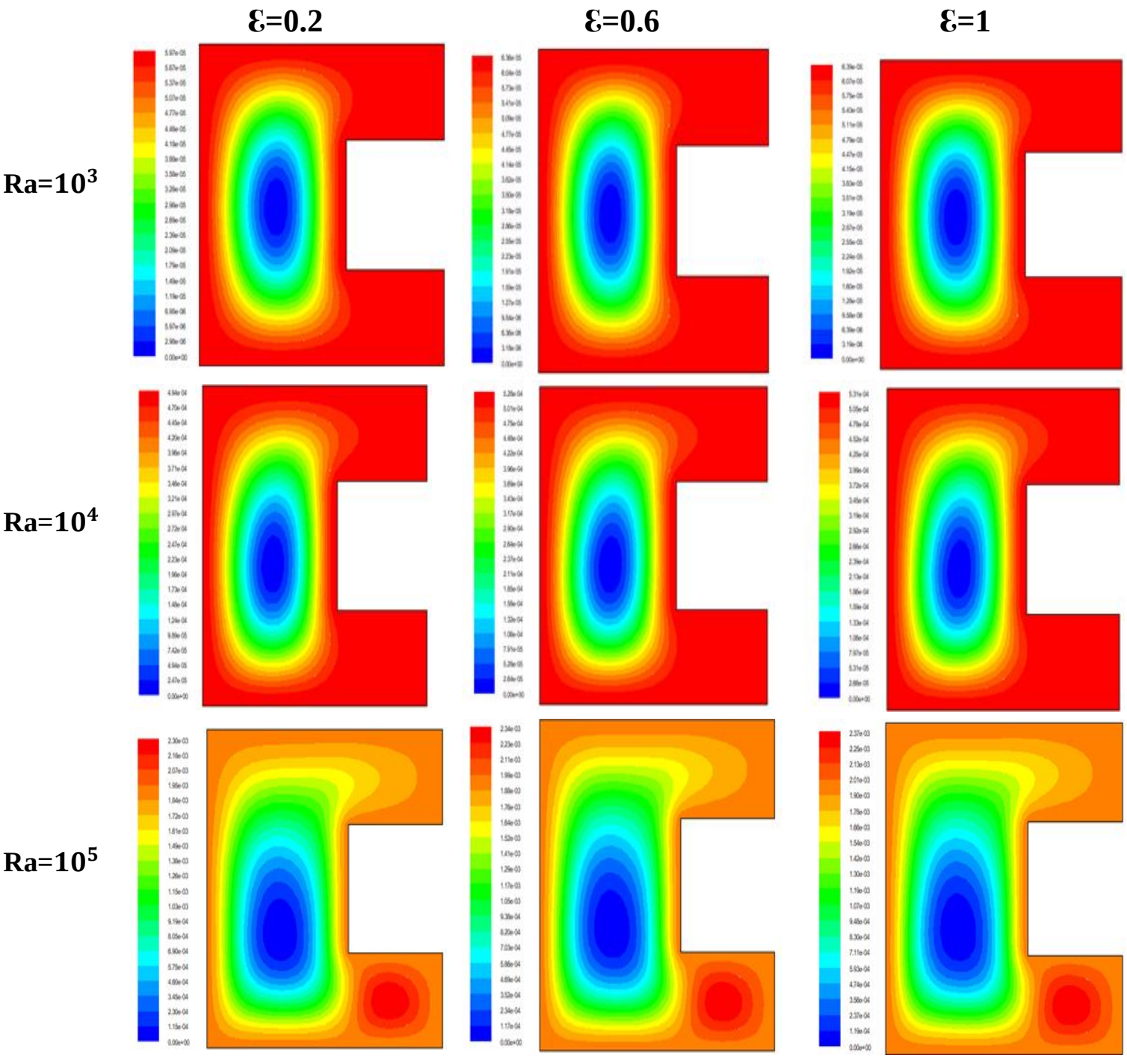

Figure III.5.: Streamlines for (Ɛ =0.2,0.6, to Ra=10^3 at 10^5) and AR=0.4

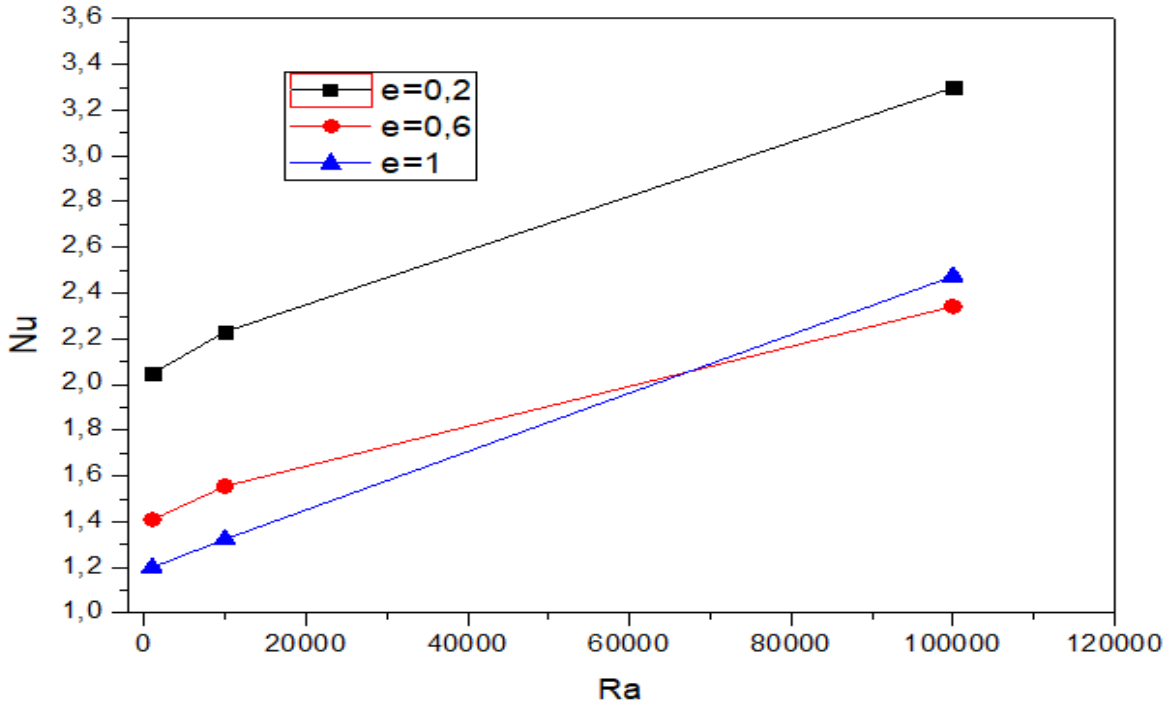

Figure III.6: Variation of average Nusselt number with the Rayleigh number for different heat portions Ɛ=0.2, Ɛ=0.6, Ɛ=1

III.3.2 Study of the influence of the aspect ratio:

In this section, the influence of the aspect ratio will be examined. The heating portion is fixed at 1, while the Rayleigh number is varied by Ra = (10^3, 10^4. 10^5) and the aspect ratio is varied by AR (0.2, 0.6, 0.8) with a Prandtl number equal to 6.2.

Figures III 7: depicts the isotherms as a function of the aspect ratio, for Rayleigh numbers ranging from Ra = 10^3 to 10^5, with a Prandtl number equal to 6.2 and the heating portion fixed at 1.

Conductive heat transfer is always present at Ra=10^3, but disappears as the Rayleigh number increases. This is due to the increased effect of buoyancy. which leads to the appearance of convective heat transfer.

For AR = 0.8, the flow pattern does not develop due to the small gap between the hot bottom wall and the cold rib, which limits the flow, and enhanced the transfer rate hence the higher Nusselt number

In addition, as the C-shaped enclosure becomes narrower, flow movement is restricted, and the Rayleigh number and buoyancy force in the area between the cold rib and the bottom wall

decrease, respectively, as the aspect ratio decreases and the Rayleigh number increases, flow is more distributed, buoyancy force increases, and flow velocity increases, as we observe, denser fluid moves downward and less dense parts upward as a function of wall temperature.

Figures III 8 shows the streamlines for the heating portion is fixed at 1, while the Rayleigh number is varied by Ra = (10^3, 10^4. 10^5), and the aspect ratio is varied by AR= (0.2, 0.6, 0.8) with a Prandtl number equal to 6.2.

Illustrates the effect of Rayleigh enhancement on flow pattern and temperature distribution

As it can be seen from the flow lines in the figure, for AR=0.2, the fluid is heated by the hot walls and expands as it rises, moving upwards. Then, the fluid is cooled by the cold walls and compresses as it descends. As a result, a clockwise vortex is created throughout the enclosure.

Moreover, as can be seen from the increase in AR, the streamlines do not appear in the central core of the C-shaped enclosure, nor do they appear below the cold wall of the cavity. This is due to the existence of a small gap between the hot and cold walls, which limits the influence of air currents, between the hot and cold walls, and limits the movement of the flow, particularly for AR = 0.8. where the isotherms are not parallel to the walls and thermal boundary layers form near the vertical walls.

Figures III 9 shows the variation of average Nusselt number with the Rayleigh number for AR=0.2, AR=0.6, AR=0.8. We observe that the Nusselt number increases with increasing aspect ratio and Rayleigh number. This explains why, when the aspect ratio decreases, the transfer rate decreases, and therefore the Nusselt number decreases.

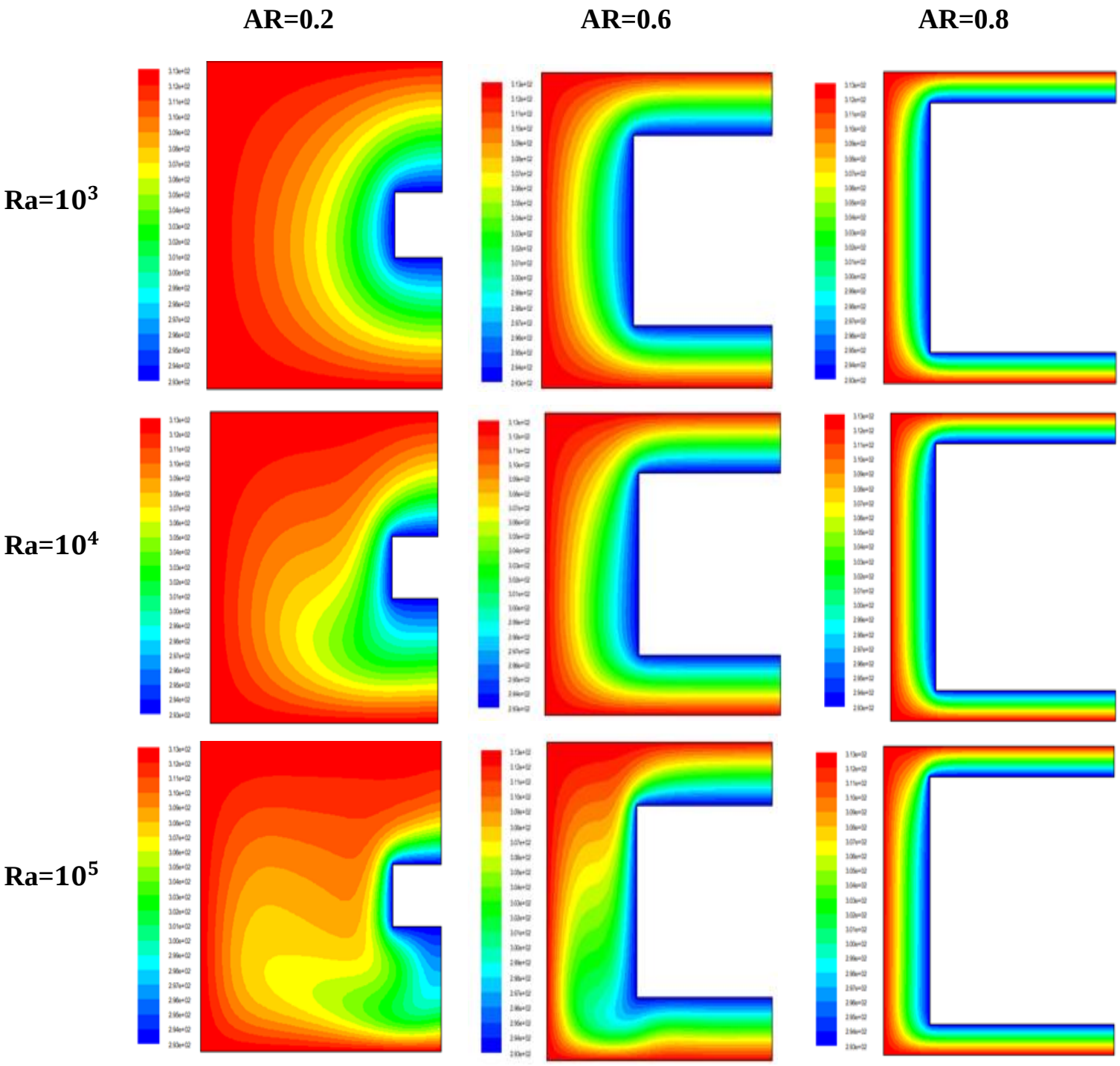

Figure III.7. Isotherms for (AR=0.2,0.6,0.8 to Ra=10^3 at 10^5) and e=1

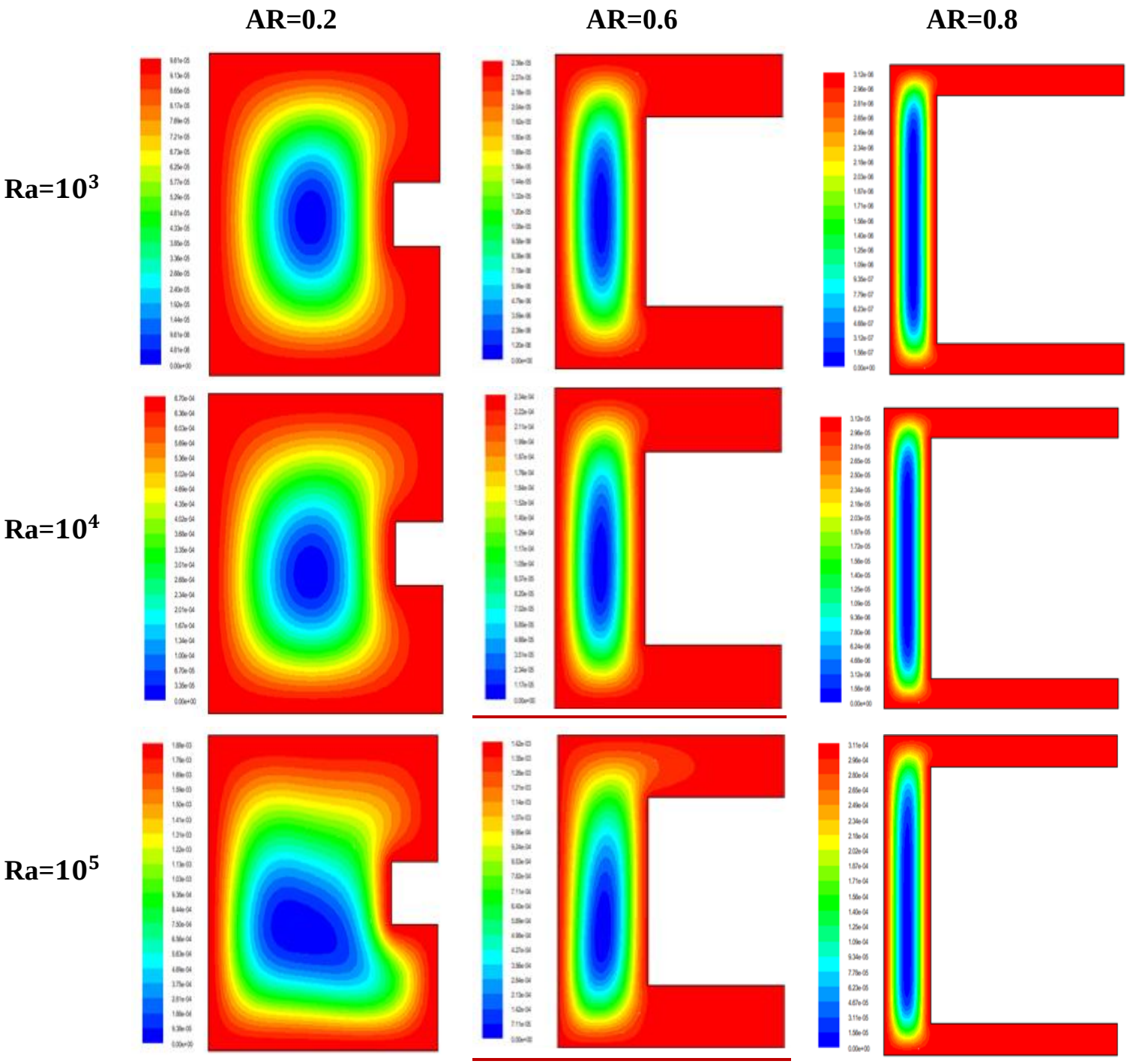

Figure III.8.: Streamlines for (AR=0.2,0.6,0.8 to Ra=10^3 at 10^5) and e=1

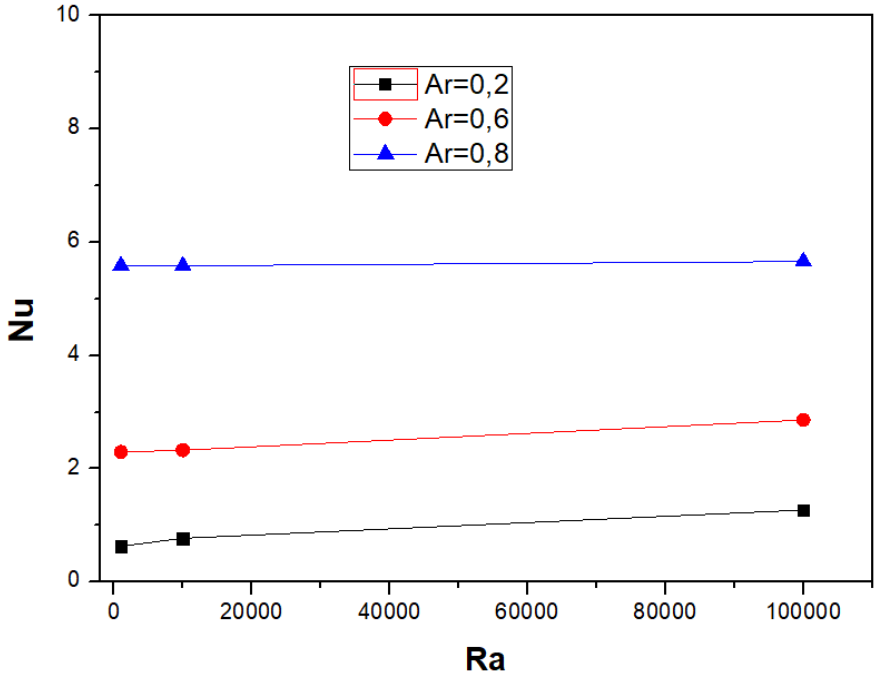

Figure III.9: Variation of average Nusselt number with the Rayleigh number for AR=0.2, AR=0.6, AR=0.8

III.3.3 Study of the influence of the Prandtl number:

In this section, the influence of the Prandtl number will be examined. The Rayleigh number being varied from 10^3 to 10^5 while varying the Prandtl number from Pr = (0.1, 1,7 and 10) with an aspect ratio equal to 0.4.

Figures III 10: depicts the streamlines as a function of the Rayleigh number being fixed initially at 10^3, 10^4 and 10^5while varying the Prandtl number from Pr = (0.1, 1,7 and 10) with an aspect ratio equal to 0.4.

When varying Prandtl number, isothermal deformation is observed to increase with increasing Prandtl number and Rayleigh number. However, the effect in the first case is relatively minor, whereas in the other cases the flow occupies a large proportion of the cavity, particularly at Pr =10. The reason is that the thermal boundary layer is diminished in the fluid with a high Prandtl number. Between the cold and hot walls on the left-hand side, a shock wave occurs between the cold and hot fluids, resulting in the formation of a feather that deforms as the Rayleigh number increases.

As the Prandtl number increases, the viscosity increases while its density decreases. This is the reason for the observed increase in the flow motion, particularly at Pr=10, and the continued deformation to increase under the influence of Rayleigh and temperature gradient.

Figures III 11: shows the streamlines as The Rayleigh number being fixed initially at 10^3, 10^4 and 10^5 while varying the Prandtl number from pr = (0.1, 1.7 and 10) with an aspect ratio equal to 0.4.

It can be observed that the speed of flow increases with an increasing Rayleigh number. Additionally, under the influence of temperature, a vortex is formed that deforms with an increasing Rayleigh number. at the same time, with an increasing Prandtl number, the vortex splits into two opposing vortices ((counter-rotating). In particular, when Ra=10^5, the large vortex rotates in a clockwise direction, while the small vortex rotates in a counterclockwise direction. In other instances, a single vortex is formed, rotating in a clockwise direction. This phenomenon can be explained by the fact that a fluid with a lower Prandtl number has a higher density.

Figures III 12 Variation of the average Nusselt number with the Rayleigh number for Pr=0.1, Pr=1, Pr=7, Pr=1. It can be seen that the average Nusselt number increases as the Rayleigh number increases, and that the change of Nusselt number as the Prandtl number changes is almost stable, but at Ra=10000 and Pr=0.1 the Nusselt value is small and as Prandtl increases it stabilizes (slight change).

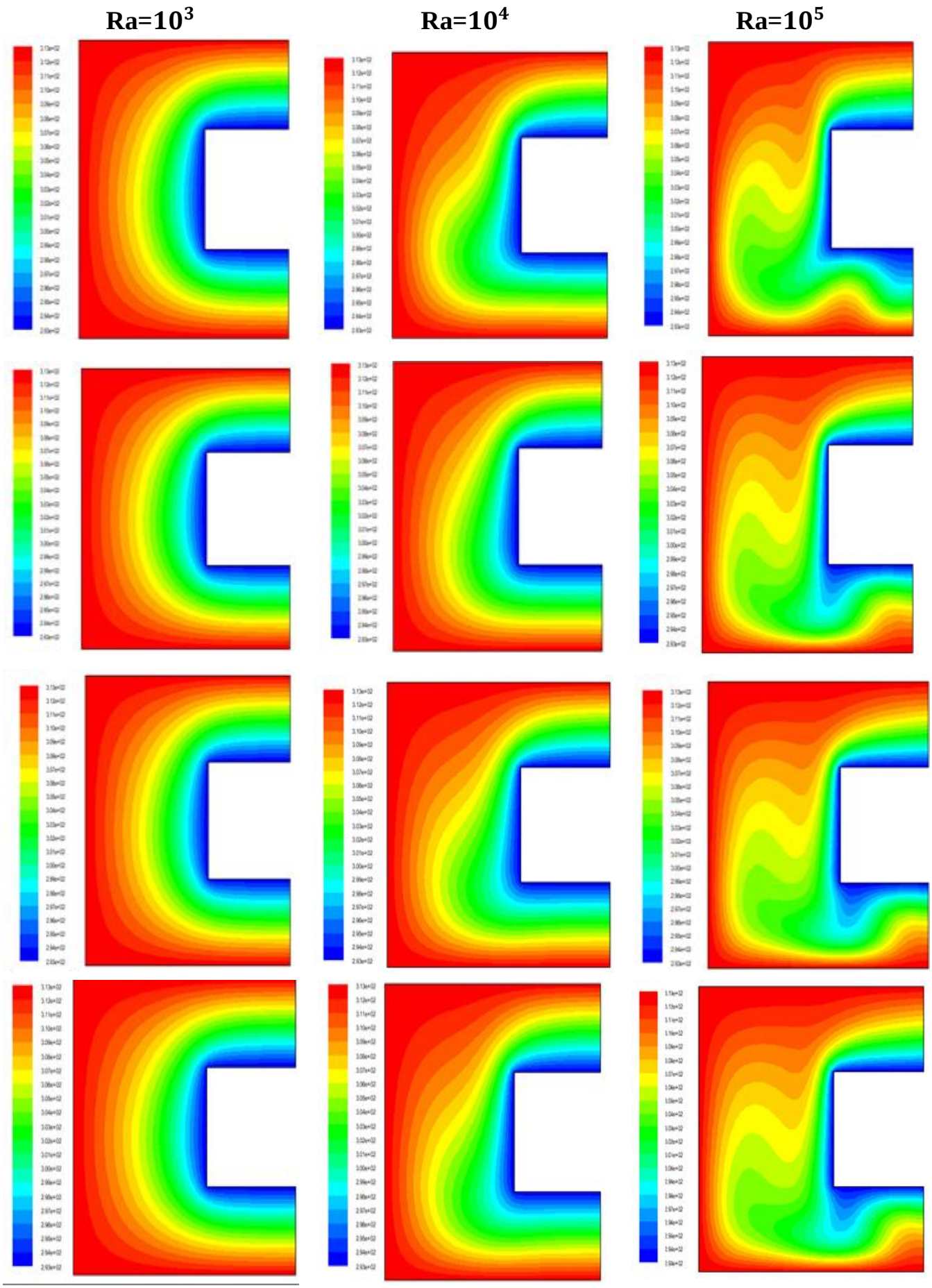

Figure III.10. Isotherms for (Pr=0.1,1,7,10 to Ra=10^3 at 10^5) and AR=0.4

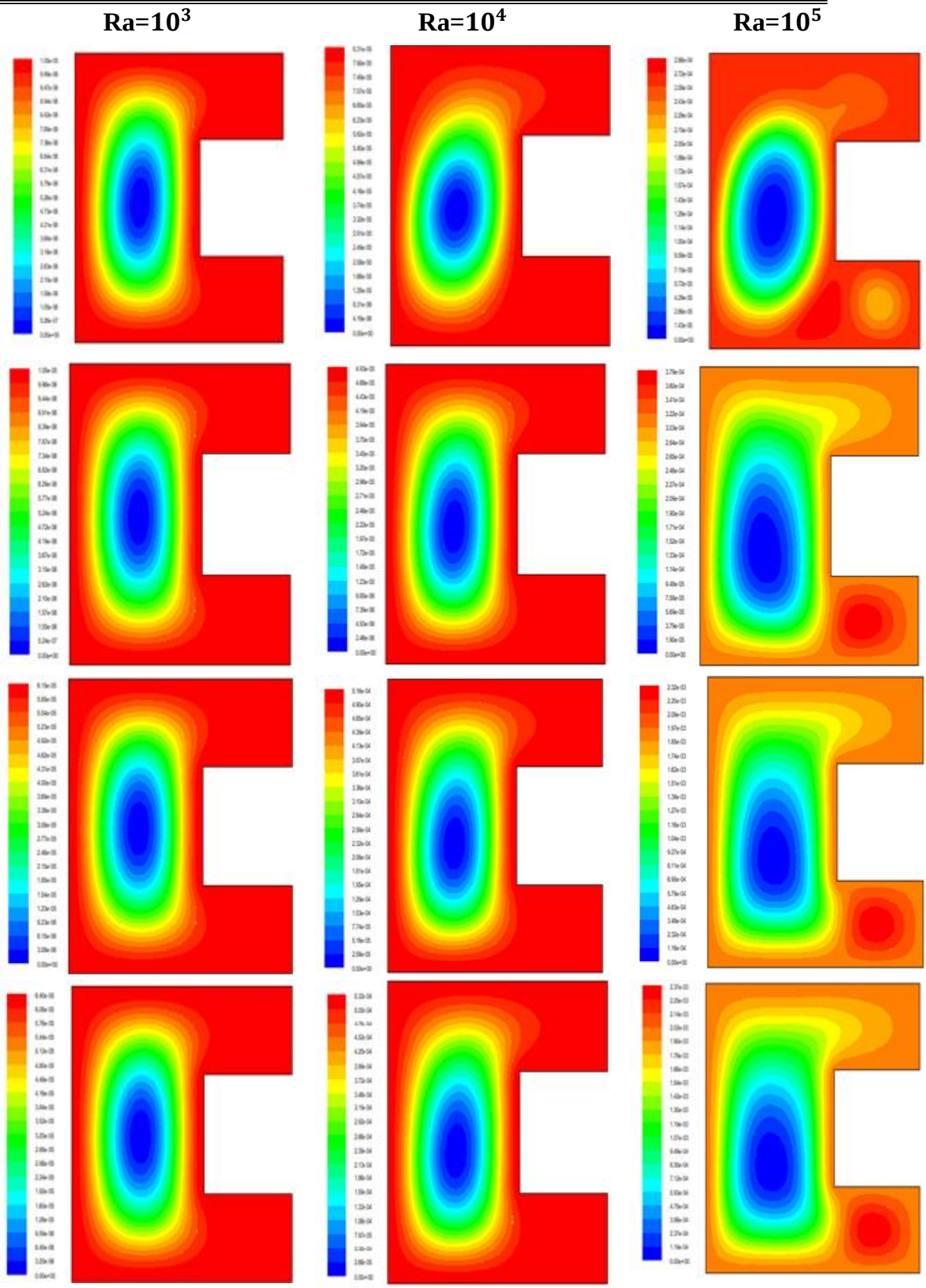

Figure III.11.: Streamlines for (Pr=0.1,1,7,10 to Ra=10^3 at 10^5) and AR=0.4

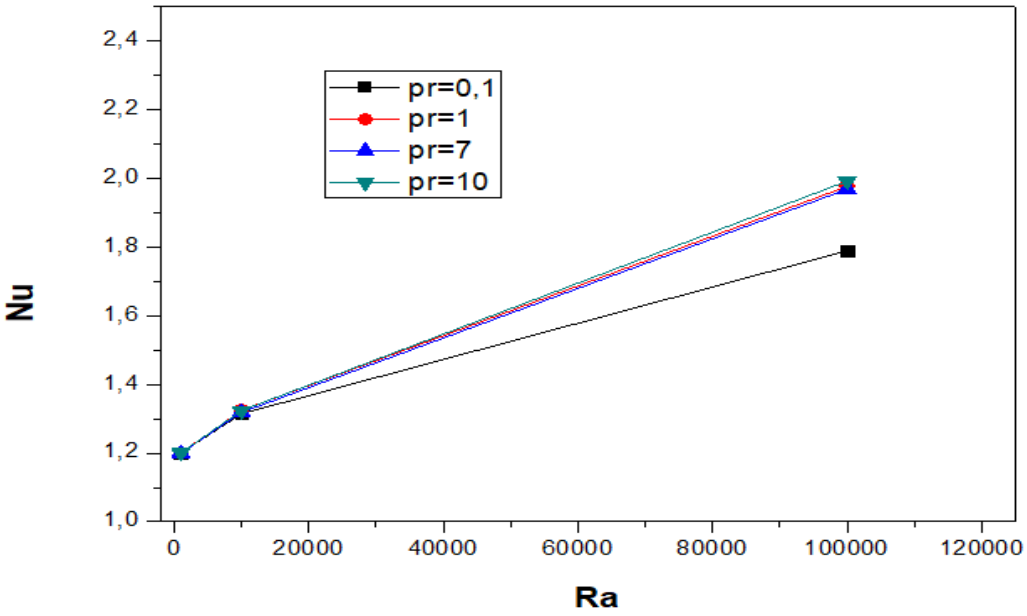

Figure III.12: Variation of the average Nusselt number with the Rayleigh number For Pr=0.1, Pr=1, Pr=7, Pr=1

III.4 Conclusions:

In this chapter we have presented the results obtained by simulating our problem, which consists of studying natural convection in a cavity formed by C

We began by validating the results obtained with the literature for classical cases of natural convection. We then studied the influence of the Rayleigh and Prandtl numbers on the different flow structures, presenting and discussing the results obtained.

We found that the variation in the heating portion, Rayleigh number, aspect ratio and Prandtl number have a considerable effect on the different flow structures. Moreover, when increasing the Rayleigh number, the aspect ratio and the Prandtl number leads to an increase in the average Nusselt number and heat transfer. However, an increase in heating portion leads to a decrease in heat transfer.

General Conclusion

In this thesis we have presented a two-dimensional numerical study of natural convection in a C-shaped cavity. The top, bottom and left walls are maintained at hot temperature, and the inner facets of the cavity at cold temperature, while the side walls are considered to be adiabatic, and this for different Prandtl and Rayleigh numbers with the aspect ratio and heating portion.

The equations governing the flow are the continuity, momentum and energy equations, and the finite volume method is used to discretize the equations. After designing the geometry using Gambit software, we moved on to steady-state numerical simulations using the commercial code Fluent. Simulation results are presented for Rayleigh numbers ranging from $10^3$to $10^5$for different heating portion and aspect ratio, and for Prandtl numbers of (Pr = 0.1, 1, 7 and 10) with an optimal mesh we chose when validating our results with the literature.

The results obtained show that:

- Increased Rayleigh number increases the average Nusselt number.
- Decreasing heating portion leads to an increase in the average Nusselt number.
- Thinner boundary layers can lead to higher transfer rates due to more efficient heat transfer between fluid and surface.
- Increasing the Prandtl number increases heat transfer.

Reference:

1) Tirth, Vineet & Pasha, Amjad & Tayebi, Tahar & Dogonchi, A & Irshad, Kashif & Chamkha, Ali & Algahtani, Ali & Al-Mughanam, Tawfiq & Galal, Ahmed. (2023). Magneto double-diffusive free convection inside a C-shaped nanofluid-filled enclosure including heat and solutal source block. Case Studies in Thermal Engineering. 45. 10.1016/j.csite.2023.102942.
2) Kalidasan, K. & Velkennedy, R. & Kanna, P. (2017). Laminar natural convection of Copper - Titania/Water hybrid nanofluid in an openended C - shaped enclosure with an isothermal block. Journal of Molecular Liquids. 246. 10.1016/j.molliq.2017.09.071.
3) Mliki, Bouchmel & Abbassi, Mohamed Ammar & Omri, Ahmed & Zeghmati, B. (2016). Lattice Boltzmann analysis of MHD natural convection of CuO-water nanofluid in inclined C-shaped enclosures under the effect of nanoparticles Brownian motion. Powder Technology. 308. 10.1016/j.powtec.2016.11.054.
4) Rahimi, A., Dehghan Saee, A., Baghban, A., Kasaeipoor, A., Ashrafi, H., & Malekshah, E. (2018). Double-MRT lattice Boltzmann simulation of natural convection in a C-shaped heat exchanger. Powder Technology, 336, 465-480.
5) Makulati, N. & Kasaeipoor, Abbas. (2016). Numerical Study of Natural Convection of a Water-Alumina Nanofluid in Inclined C-Shaped Enclosures under the Effect of Magnetic Field. Advanced Powder Technology. 27. 661–672. 10.1016/j.apt.2016.02.020.
6) Nayak, Manoj & Karimi, Nader & Chamkha, Ali & Dogonchi, A. & El-Sapa, Shreen & Galal, Ahmed. (2022). Efficacy of diverse structures of wavy baffles on heat transfer amplification of double-diffusive natural convection inside a C-shaped enclosure filled with hybrid nanofluid. Sustainable Energy Technologies and Assessments. 53. 102180.
7) Asha, Nur & Molla, Md. (2023). MRT-lattice Boltzmann simulation of MHD natural convection of Bingham nanofluid in a C-shaped enclosure with response surface analysis. Heliyon. 9. e22539. 10.1016/j.heliyon.2023. e 22539.
8) Mansour, M. & Armaghani, Taher & Chamkha, Ali & Rashad, A. (2019). Entropy generation and nanofluid mixed convection in a C-shaped cavity with heat corner and inclined magnetic field. The European Physical Journal Special Topics. 228. 2619-2645. 10.1140/epjst/e2019-900050-3.
9) Mojumder, Satyajit & Saha, Sourav & Saha, Sumon & Mamun, Mohammad. (2014). Effect of Magnetic Field on Natural Convection in a C-shaped Cavity Filled with

Ferrofluid. Procedia Engineering. 105. 10.1016/j.proeng.2015.05.012.

10) Mahmoodi, Mostafa & Hashemi, Seyed. (2012). Numerical study of natural convection of a nanofluid in C-shaped enclosures. International Journal of Thermal Sciences. 55. 76–89. 10.1016/j.ijthermalsci.2012.01.002.

11) Armaghani, Taher & Esmaeili, Hossein & Mohammadpoor, Y. & Pop, I. (2018). MHD mixed convection flow and heat transfer in an open C-shaped enclosure using water-copper oxide nanofluid. Heat and Mass Transfer. 54. 10.1007/s00231-017-2265-3.

12) Abedini, A. & Armaghani, Taher & Chamkha, Ali. (2018). MHD free convection heat transfer of a water–Fe3O4 nanofluid in a baffled C-shaped enclosure. Journal of Thermal Analysis and Calorimetry. 135. 10.1007/s10973-018-7225-8.